SAND-76-0061
UNLIMITED RELEASE

NUMERICAL INTEGRATION OF A SPALL-DAMAGE VISCOPLASTIC CONSTITUTIVE MODEL IN A ONE-DIMENSIONAL WAVE PROPAGATION CODE

M. E. Kipp and A. L. Stevens

Prepared by Sandia Laboratories, Albuquerque, New Mexico 87115 and Livermore, California 94550 for the United States Energy Research and Development Administration under Contract AT (29-1)-789

Printed June 1976

Sandia Laboratories

SF 2900 Q(7-73)

When printing a copy of any digitized SAND Report, you are required to update the markings to current standards.

Issued by Sandia Laboratories, operated for the United States Energy Research & Development Administration by Sandia Corporation.

NOTICE

This report was prepared as an account of work sponsored by the United States Government. Neither the United States nor the United States Energy Research & Development Administration, nor any of their employees, nor any of their contractors, subcontractors, or their employees, makes any warranty, express or implied, or assumes any legal liability or responsibility for the accuracy, completeness or usefulness of any information, apparatus, product or process disclosed, or represents that its use would not infringe privately owned rights.

Printed in the United States of America
Available from
National Technical Information Service
U. S. Department of Commerce
5285 Port Royal Road
Springfield, VA 22151
Price: Printed Copy $5.50; Microfiche $2.25

SAND-76-0061
Unlimited Release
Printed June 1976

NUMERICAL INTEGRATION OF A SPALL-DAMAGE VISCOPLASTIC CONSTITUTIVE MODEL IN A ONE-DIMENSIONAL WAVE PROPAGATION CODE

M. E. Kipp
Computational Physics & Mechanics Division I - 5162

and

A. L. Stevens
Oil Shale Programs Division 5734
Sandia Laboratories, Albuquerque, New Mexico 87115

ABSTRACT

A description is given of the incorporation of a model for spall damage in ductile metals into the WONDY one-dimensional Lagrangian wavecode. The constitutive equations modeling the thermomechanical behavior of the damaged viscoplastic material are given as a system of seven first order ordinary differential equations. In any zone-cycle, these equations are integrated by the variable order, variable step Adams-method code, STEP1.

Sample calculations for a plane impact case illustrate the interaction of the accumulating damage with the stress wave. Included are brief parameter studies which indicate the dependence of the damage on the viscoplastic model. Back surface velocity histories are compared with experimental records.

I. INTRODUCTION

The elastic-viscoplastic-damage constitutive model described by Davison, et. al. [1], may be numerically evaluated within the existing structure of a wavecode. It is the purpose of this report to delineate the incorporation of this model into the one-dimensional Lagrangian wavecode, WONDY [2]. The order of computations in WONDY is such that the equation of motion (conservation of momentum) and constitutive model (with conservation of energy) are staggered in time. Hence, for a given mass element or zone of material, the equation of state routine, which contains the constitutive model, is entered after the density of the zone has already been determined from the motion equation for a prescribed timestep. The equation of state routine must then compute the corresponding stresses and energy, and remaining state variables, corresponding to this new density or strain. The constitutive model is essentially integrated in time, from its old values to its new ones (at the end of the timestep) whether it be by differencing, as is conventionally the case, or by formally (numerically) integrating, as will be done here.

Solution of the constitutive and energy equations is not amenable to a difference scheme applied across the timestep for this model, primarily because of the complexity of coupling involved among variables. The choice remaining is that of numerical integration of the equations. One approach involves defining an integrator that subcycles within the prescribed code timestep using a crude difference scheme, and dividing the cycle into more and more uniform subcycles until some sort of convergence occurs. This has been attempted with inconsistent and unsatisfactory results. The alternative has been the successful use of the external

integrator STEP1 [3] (a variable order, variable step, Adams-method differential equation solver) to integrate the constitutive model within specified error tolerances.

In order to maintain perspective, the constitutive model equations, in plane symmetry, will be reproduced in full in Section II. A discussion of the actual incorporation of these equations into WONDY is found in Section III, and the use of the integrator STEP1 is outlined in Section IV. Section V is devoted to example calculations that indicate the effects of various features of the model on the solution of typical problems. The final section, VI, contains the conclusions of this report. Appendices are included listing the WONDY data arrays, coding of the constitutive model, required minimum updates to utilize this model in WONDY, and specific material data for the sample calculations.

II. EQUATIONS FOR THE VISCO-PLASTIC-DAMAGE MODEL

For the purpose of clarifying the insertion of the elastic-viscoplastic-damage model into WONDY, it is useful to reconstruct the one-dimensional theory of uniaxial strain given in [1]. The direction 33 has been designated the longitudinal (axial) direction, and 11 and 22 the transverse directions. The motion $\underset{\sim}{x}$ is defined to be

$$\underset{\sim}{x} = (X_1, X_2, \hat{x}(X_3, t)) \tag{1}$$

where the deformation gradient ($\underset{\sim}{F}$) is equal to the product of the elastic deformation ($\underset{\sim}{E}$), spall dilation ($\underset{\sim}{M}$), and viscoplastic slip ($\underset{\sim}{P}$). The specific components of the deformation gradient are

$$F = \frac{\partial \hat{x}}{\partial X_3} = F_{33} = E_{33}\, M\, P_{33} \tag{2a}$$

and

$$1 = F_{11} = F_{22} = E_{11}\, M\, P_{11} \; . \tag{2b}$$

The spall dilatation M is related to the damage $\mathcal{D}$ by

$$M = 1/(1 - \mathcal{D})^{1/3} \; ; \tag{3}$$

the plastic deformation is isochoric, that is,

$$(P_{11})^2 P_{33} = 1 \; , \tag{4}$$

so the elastic deformations may be expressed as

$$E_{11} = \sqrt{P_{33}}\, (1 - \mathcal{D})^{1/3} \tag{5a}$$

$$E_{33} = \frac{F}{P_{33}}\, (1 - \mathcal{D})^{1/3} \; . \tag{5b}$$

The elastic strains are defined to be

$$e_{11} = E_{11} - 1 \tag{6a}$$

$$e_{33} = E_{33} - 1 \tag{6b}$$

so that for small strains, the stress response is

$$\begin{aligned} t_{11} &= 2(\kappa + \tfrac{1}{3}\mu)e_{11} + (\kappa - \tfrac{2}{3}\mu)e_{33} - 3\alpha\kappa(\theta - \theta_R) \\ t_{33} &= 2(\kappa - \tfrac{2}{3}\mu)e_{11} + (\kappa + \tfrac{4}{3}\mu)e_{33} - 3\alpha\kappa(\theta - \theta_R) \end{aligned} \tag{7}$$

where α is the thermal coefficient of expansion, θ is the temperature and θ_R is the reference temperature. The elastic constants are modified by the damage to become

$$\begin{aligned} \kappa &= \kappa_o\left[1 - \frac{3(1 - \nu_o)}{2(1 - 2\nu_o)}\mathcal{D}\right] \\ \mu &= \mu_o\left[1 - \frac{15(1 - \nu_o)}{7 - 5\nu_o}\mathcal{D}\right] \end{aligned} \tag{8}$$

where the Poisson's ratio is

$$\nu_o = \frac{1}{2}(3\kappa_o - 2\mu_o)/(3\kappa_o + \mu_o) .$$

The average stress is defined to be

$$\sigma = \frac{1}{3}(2t_{11} + t_{33}) = \kappa\left[2e_{11} + e_{33} - 3\alpha(\theta - \theta_R)\right] . \tag{9}$$

The nucleation and growth of voids to produce damage is governed by the following equations: void nucleation rate is given by

$$\dot{n} = C_n\left\{\exp\left[\frac{\sigma - \sigma_n + |\sigma - \sigma_n|}{2\sigma_1}\right] - 1\right\} \tag{10}$$

and the rate of damage accumulation is determined from

$$\dot{\mathcal{D}} = \dot{n}\mathcal{V}_o(1 - \mathcal{D})^2 + \frac{3}{2} C_G\left[2\sigma + \left|\sigma - \sigma_G\right| - \left|\sigma + \sigma_G\right|\right]\mathcal{D}(1 - \mathcal{D}) \ . \tag{11}$$

The required damage parameters are C_n (nucleation rate coefficient), σ_n (nucleation threshold), σ_1 (nucleation stress sensitivity parameter), $\mathcal{V}_o$ (initial volume of an individual void), C_G (growth rate coefficient), and σ_G (growth threshold). n is the total number of voids, and $\mathcal{D}$ is the void volume fraction.

In the plane case, the viscoplastic response requires a maximum resolved shear stress, given as

$$\tau = \mu(e_{33} - e_{11})/(1 - \mathcal{D})^{2/3} \ . \tag{12}$$

The plastic deformation gradient is

$$\dot{P}_{33} = \frac{1}{2} B \, D_{(T)} \, f_{(m)} \, V(\tau) P_{33} \tag{13}$$

where the dislocation density is determined from

$$\dot{D}_{(T)} = A^*(D^*_{(T)} - D_{(T)})D_{(T)} \, f_{(m)} \left|V(\tau)\right| \ . \tag{14}$$

The mobile fraction of these dislocations is determined from

$$\dot{f}_{(m)} = -B^* D_{(T)}(f_{(m)} - f^*_{(m)})f_{(m)}V(\tau) \tag{15}$$

and the average velocity of mobile dislocations is taken to be

$$V(\tau) = \begin{cases} 0 \ , & |\tau| \le \tau_{(A)} \\ \sqrt{\dfrac{\mu}{\rho_R}} \ \mathrm{sgn}\ (\tau) \ \dfrac{s^m}{1 + s^m} \ , & |\tau| > \tau_{(A)} \end{cases} \tag{16}$$

where

$$s = (|\tau| - \tau_{(A)})/\tau^* \tag{17}$$

and

$$\tau_{(A)} = \tau_{(A_o)}\left[1 + (\gamma/\gamma_o)^{1/n}\right] . \tag{18}$$

From Reference [1],

$$\dot{P}_{33} = \frac{\dot{\gamma}}{2} P_{33} ;$$

$\dot{\gamma}$ may be integrated to find the "shear strain"

$$\gamma = 2 \ \ell n \ P_{33}$$

so Eq. (18) above becomes

$$\tau_{(A)} = \tau_{(A_o)}\left[1 + \left(\frac{2}{\gamma_o} \ \ell n \ P_{33}\right)^{1/n}\right] . \tag{19}$$

The constants required in the viscoplastic equations are B (the Burgers' length), A^*, $D^*_{(T)}$ (saturation dislocation density), B^*, $f^*_{(m)}$ (saturation mobile fraction), m, τ^*, $\tau_{(A_o)}$ (yield stress), γ_o, and n.

Finally, the energy equation (Eq. (102) in [1]) is written in terms of the temperature to be

$$\begin{aligned}\dot{\theta} = \Big\{ & -\mathrm{div}\ \underset{\sim}{q} + \rho_R(1 - \mathcal{D})(1 - \underset{\sim}{I_e})r + 0.9\ \mathrm{tr}(\underset{\sim}{t}\ \underset{\sim}{L}^{(P)}) \\ & - 3\alpha\kappa\theta_R\ \underset{\sim}{\dot{I}_e} - \left[3\alpha\theta_R\left(\kappa' + \frac{\kappa}{1 - \mathcal{D}}\right) \underset{\sim}{I_e} - \alpha^2\kappa'(1 - \mathcal{D})\theta_R(\theta - \theta_R)\right. \\ & \left. - (\sigma - Q_T)/(1 - \mathcal{D})\right]\dot{\mathcal{D}}\Big\}/(1 - \mathcal{D})(\underset{\sim}{C_t}\rho_R - \alpha^2\kappa\theta_R)\end{aligned} \tag{20}$$

where

$$I_{\underset{\sim}{e}} = 2e_{11} + e_{33}$$

$$\kappa' = -\kappa_o \frac{3(1 - \nu_o)}{2(1 - 2\nu_o)}$$

$$\mathrm{tr}(\underset{\sim}{t}\, \underset{\sim}{L}^{(P)}) = (t_{33} - t_{11} - Q_T)\dot{P}_{33}/P_{33}$$

$$\dot{I}_{\underset{\sim}{e}} = 2\dot{E}_{11} + \dot{E}_{33} = 2E_{11}\left[\frac{\dot{P}_{33}}{2P_{33}} - \frac{\dot{\mathcal{D}}}{3(1 - \mathcal{D})}\right] - E_{33}\left[\frac{\dot{\rho}}{\rho_T} + \frac{\dot{P}_{33}}{P_{33}} + \frac{\dot{\mathcal{D}}}{3(1 - \mathcal{D})}\right].$$

In addition, $\underset{\sim}{q}$ is the heat flux, r is the radiation term, $C_{\underset{\sim}{t}}$ is the specific heat at constant stress, Q_T is the artificial viscosity, and ρ_T is the density of the medium.

A parallel energy equation in terms of the specific internal energy is maintained, taking the form

$$\dot{\varepsilon} = r - \frac{1}{\rho_T} \operatorname{div} \underset{\sim}{q} - (t_{33} - Q_T)\dot{\rho}/\rho_T^2 \tag{21}$$

The equations provided here are specifically derived for the case of uniaxial strain. A more general version could be written, but it is felt that for one dimension, uniaxial strain is the most commonly encountered case, and the simplest for verifying the model; other interesting cases involve two dimensions, to which the general equations in [1] may be reduced.

III. WONDY - STATE 5

In the WONDY wavecode, the order of operation is such that the time-step required for numerical stability is specified in terms of the parameters associated with the previous cycle. For a given zone, the density associated with the end of this timestep is first determined, and the equation of state routine is then used to calculate the stresses, internal energy, and other variables which may be required.

With respect to the present constitutive model, the deformation gradient F_{33} for any zone is equal to the ratio of the reference density, ρ_R, to the new density, ρ_N. Equations (2-8) are evaluated to obtain the stresses, after which the derivative evaluations are performed, Eqs. (9-21). There are seven coupled ordinary differential equations to be integrated for the variables:

- η - number density of voids, Eq. (10),
- $\mathcal{D}$ - damage (void volume fraction), Eq. (11),
- $D_{(T)}$ - dislocation density, Eq. (14),
- $f_{(m)}$ - fraction of mobile dislocations, Eq. (15),
- P_{33} - axial plastic deformation gradient, Eq. (13),
- θ - temperature, Eq. (20), and
- ϵ - internal energy, Eq. (21).

Of these seven variables, η and ϵ are not explicitly used in the derivative evaluations or stress determination. The number density, η, is used only in derivative form in the damage equation (11). Hence, in terms of material response, a redundant but physically interesting damage parameter is being evaluated. Maintaining the product $C_\eta \mathcal{V}_o$ constant produces fixed damage levels (Eq. (10,11)); the purpose of C_η

is to adjust the number density to match post-mortem experimental evidence. Since the WONDY wavecode carries an internal energy check, Eq. (21) for the internal energy is required; it is also included in the model in case future modifications in stress-strain behavior would require use of the internal energy instead of the temperature.

Under normal conditions, the initial values of the variables are set to reflect an unstressed, unstrained, quiescent medium. The variables η, $\mathcal{D}$, P_{33}, and ϵ are then initialized to zero, zero, one, and zero, respectively. A reference temperature, θ_R, is needed, as is an initial dislocation density and an initial fraction of mobile dislocations. It is apparent, however, that one may just as easily begin with a predamaged material, say, and enter an initial damage distribution.

In addition to the normal variables carried for each zone in the wavecode, (which includes the internal energy, ϵ), the remaining six variables are stored for each zone. For any timestep, the previous values are taken as initial data, and integrated in time to the end of the timestep, resulting in new values for each variable. Since the density has already been determined for the end of the timestep, it must be modified to a linear function of time across the timestep to permit proper integration for the seven variables. Denoting ρ_o and ρ_N as old and new densities corresponding to times T_o and T_N, the density ρ_T can then be expressed as

$$\rho_T = \frac{\rho_N - \rho_o}{T_N - T_o} (T - T_o) + \rho_o \tag{22}$$

A similar situation exists for the code's artificial viscosity, which appears only in the energy equation. This linear function takes the form

$$Q_T = \frac{Q_N - Q_o}{T_N - T_o} (T - T_o) + Q_o \tag{23}$$

The time increment in WONDY by which a stable computation may advance each cycle depends upon the zone size, artificial viscosity, and sound speed. The sound speed is calculated in the equation of state subroutine and has been approximated by a constant value in the present case. The maximum sound speed is taken as the elastic longitudinal wave speed, and has been found to provide stable computations.

WONDY is operating with a total of seventeen variables when using the present model, and the storage arrangement for the additional variables is given in Appendix A. The material parameters for the viscoplastic and damage models are stored in an array, ESC, and their appropriate designations are also given in Appendix A.

The equation of state calculation has been placed in the subroutine STAT5. This subroutine contains a driver for the integrator STEP1. STAT5 also contains an entry point, STIN5, in which internal parameters are calculated and the new variables initialized. The subroutine F(T,$\underset{\sim}{Y}$,$\underset{\sim}{YP}$) does the derivative computations required by STEP1 to integrate the variables each zone-cycle. The coding for STAT5 and F(T,$\underset{\sim}{Y}$,$\underset{\sim}{YP}$) is given in Appendix B. The standard WONDY output has been altered, and the variables written to tape for plotting have been changed. These updates are listed in Appendix C for convenience.

The coding is quite transparent, and in such a form that major changes in material characterization may readily be effected. Differing damage models may be accommodated without any major code alterations, as may alternate stress-strain relations, etc. This flexibility is due in large part to the use of an external integrator.

IV. INTEGRATOR FOR THE EQUATIONS - STEP1

The efficient solution of the system of first order ordinary differential equations encountered in this constitutive model is mandatory. In addition, cognizance of the integration errors is desirable, and stability of the integration independent of wavecode zone sizes or timesteps is a firm requirement. Rather than attempt to build into the code a rudimentary integrator, with the incumbent task of proving it out, an existing integrator, built specifically for such systems of equations, and known to be efficient and exhaustively tested, was employed. The integrator, STEP1, documented in [3], is based upon a variable order, variable step version of the Adams PECE (Predict Evaluate Correct Evaluate) formulas. The predictor and corrector are of order k and k+1, respectively, (which is equivalent to using a kth order predictor, and corrector with local extrapolation). For stability reasons, a maximum k of twelve is imposed. Each successful call to STEP1 advances the solution of the equations one step, so the integrator is called repeatedly for each zone-cycle until the wavecode timestep has been exceeded, at which point the code INTRP [3] interpolates the variables to the proper wavecode time. (The integrator determines its most efficient timestep internally, independent of the stability criterion employed by WONDY.) The integrator is self-starting, requiring only the initial values of the variables to be integrated. The weighted local error in each variable is limited at each integration timestep to a tolerance EPS specified in the material input (Appendix A). Setting the weight to the magnitude of the variable provides a relative error. (As noted above, the number density and the internal energy are not explicitly required, so their weights have been

set very large to avoid having either of these variables control the STEP1 integration step. The remaining variables are held within relative error bounds.)

Upon return from a successful step, STEP1 has determined what the next optimum step size should be, and the proper order, k, for continuing the integration. The derivative evaluations are performed in an external subroutine F(T,$\underset{\sim}{Y}$,$\underset{\sim}{YP}$), described in Appendix B, which is required to be called twice for each successful step. The total number of calls have been monitored for the purposes of determining the efficiency of using STEP1 in this constitutive model, and for EPS of 10^{-4} (relative error), an average of 4 steps is required per zone-cycle. A check on the stiffness of the differential equations is performed, stiffness being defined as requiring 500 calls to STEP1 in a (wavecode) time interval, of which 50 consecutive calls must have order less than or equal to 4. The equations have not appeared to be stiff in problems tested to the present. It may also be noted that using this model on the CDC 6600, WONDY calculates about $5(10^5)$ zone-cycles/hour; an elastic-perfectly-plastic model in STATE1 will normally calculate at about the rate of $5(10^6)$ zone-cycles/hour, while a rate-dependent iterative model in STATE4 may calculate as slowly as $5(10^4)$ zone-cycles/hour.

V. EXAMPLES

It is the intent of this section to demonstrate the behavior of media modeled by the constitutive equations in Section II. A sampling of test problems is included to illustrate the coupling between viscoplastic and damage behavior. Specifically, the problems will demonstrate material response with and without damage being permitted to accrue, the alterations in behavior caused by the inclusion of the dislocation multiplication mechanism, and response in the face of gross zoning changes.

The back surface velocity histories are augmented by two experimental histories for the geometries to be discussed. Although a "best fit" is not the purpose here, very good agreement will be seen to exist, indicating the potential of the model for damage studies.

Two geometries in uniaxial strain will be considered. The first case (A) entails a fused quartz flyer, 3.1674 mm thick, with velocity 300.8 m/s, impacting an 1100 aluminum target, 6.3856 mm thick, backed by a fused quartz window, 13.297 mm thick. The experimental velocity history is taken at the target/window interface. The second case (B) is the impact of a fused quartz flyer, 3.178 mm thick, velocity 141.95 m/s, with an aluminum target, 6.3998 mm thick. The experimental velocity history is of the rear surface of the target. Finally, a case (C) is considered with geometry identical to that of case (B), but with coarse zoning.

In case (A), the loading wave is generated at the flyer/target impact interface. The compressive wave in the flyer reflects off the trailing free surface as a release wave, propagating back through the flyer and on into the aluminum. The window first transmits the loading wave from the aluminum, followed shortly by the release, or unloading wave. The quartz

and aluminum have slight dissimilarities of impedance, so the loading wave experiences a small reduction in magnitude as it passes through the window.

In case (B), since the aluminum has a free surface on the back face, the initial loading wave is reflected as a release wave back into the aluminum. When the release waves originating from the flyer and the back surface meet, a region of tension ensues, in which damage may form, relaxing the tension, and causing a recompression wave to drive towards the rear aluminum face. It will be seen that the viscoplastic model strongly influences the location and character of the initial tension wave that is developed, hence significantly affecting the resulting damage.

The data for the fused quartz are from [4], and are listed in Appendix D, Table 1. This material utilizes STATE 1 in WONDY for its description. The data for the aluminum are listed in Appendix D, Table 2. The initial damage parameters are from [5]. In case A, the flyer has 32 zones, the target, 64 zones, and the window, 133 zones. Case B has 30 zones in the flyer and 60 zones in the target, and case C is zoned with 6 zones in the flyer and 12 zones in the target. The problem time is 4 μs, corresponding to the experimental record history duration. In all cases, the quadratic and linear viscosity coefficients in WONDY are taken to be 0.5 and 0.25, respectively; this permits some minor oscillations to develop, but does not obscure the details of the wave front in the aluminum.

A. Fused Quartz Flyer/Aluminum Target/Fused Quartz Window

Case A-1.

In this example, the dislocation multiplication mechanism has been turned off ($A^* = -1$). Figure 1 is the target/window interface velocity history illustrating the loading and unloading behavior of the wave entering the window from the aluminum.

Case A-2.

When the above case A-1 has the dislocation multiplication turned on, ($A^* = -1.0(10^{-4})$), the precursor assumes better definition, and the arrival time of the relief wave is improved (Figure 2). The steepness of the loading wave is also a function of zone size and artificial viscosity, and much time could be spent attempting to obtain a better fit. Strain hardening is ignored and the fraction of mobile dislocations has remained fixed and this may affect the wave shape. The wave profiles at 0.5, 1.5, and 2.5 μs are shown in Figure 3. The profile at 1.5 μs shows the unloading of the wave caused by the dissimilarities in target and window impedances. Note also the oscillations at early times caused by the use of very low values of the artificial viscosity.

Case A-3.

If one were to desire to reshock a previously damaged material, or were to interpret a distended metal as uniformly "predamaged", some initial damage, $\mathcal{D}_o$, must be specified, as must be an initial density related through $\mathcal{D}_o$ to the solid density. If the initial stresses are to be zero, E_{11} and E_{33} must be unity. Since $\mathcal{D}_o$ is in fact the void volume fraction, the initial density of the expanded material is $\rho_R(1 - \mathcal{D}_o)^{1/3}$, from Eq. (2a) and $F_{11} = 1/(1 - \mathcal{D}_o)^{1/3}$, from Eq. (2b). Equation (5a) must be rewritten as

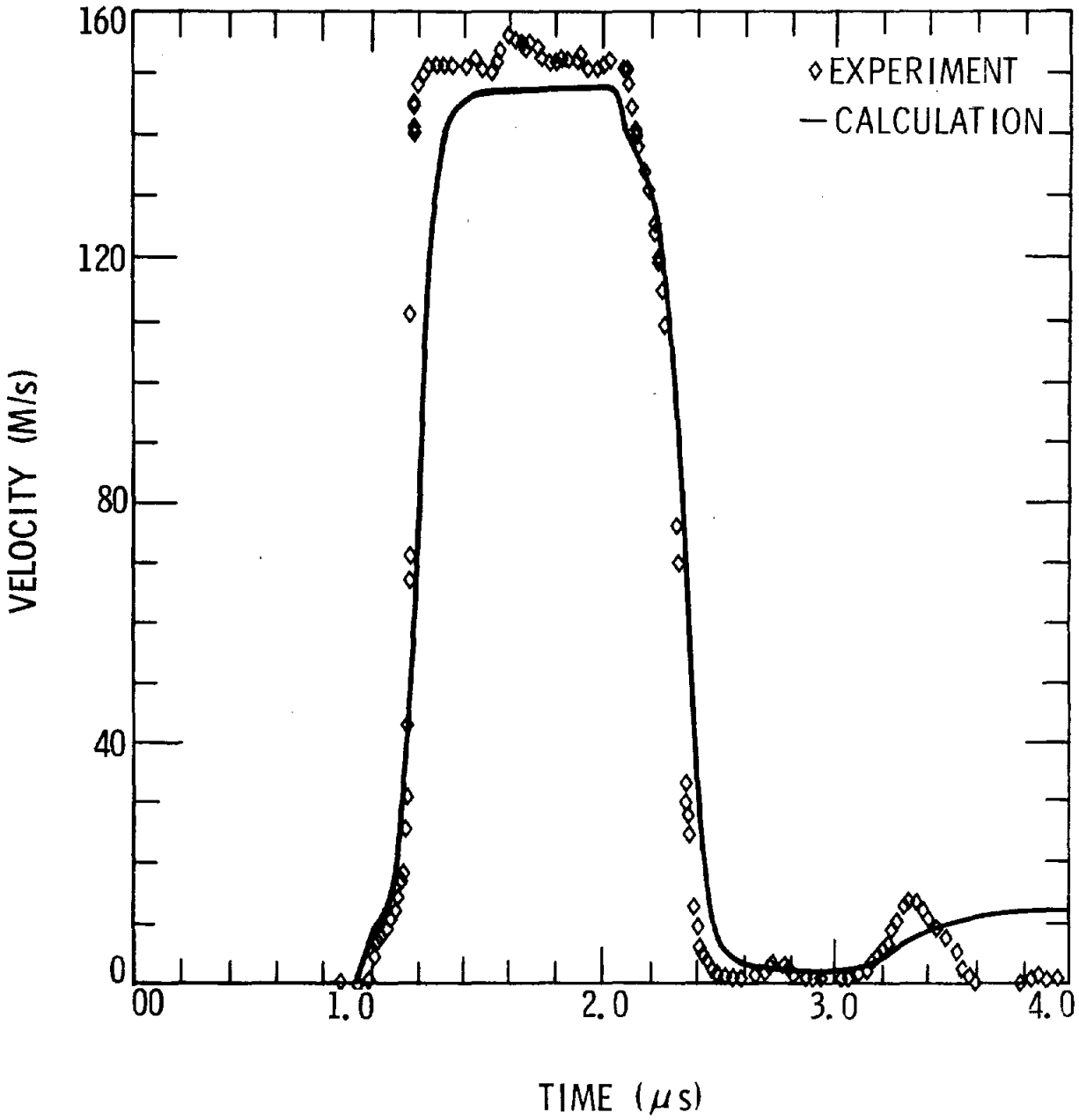

Figure 1. Aluminum/quartz interface velocity history. Dislocation multiplication suppressed.

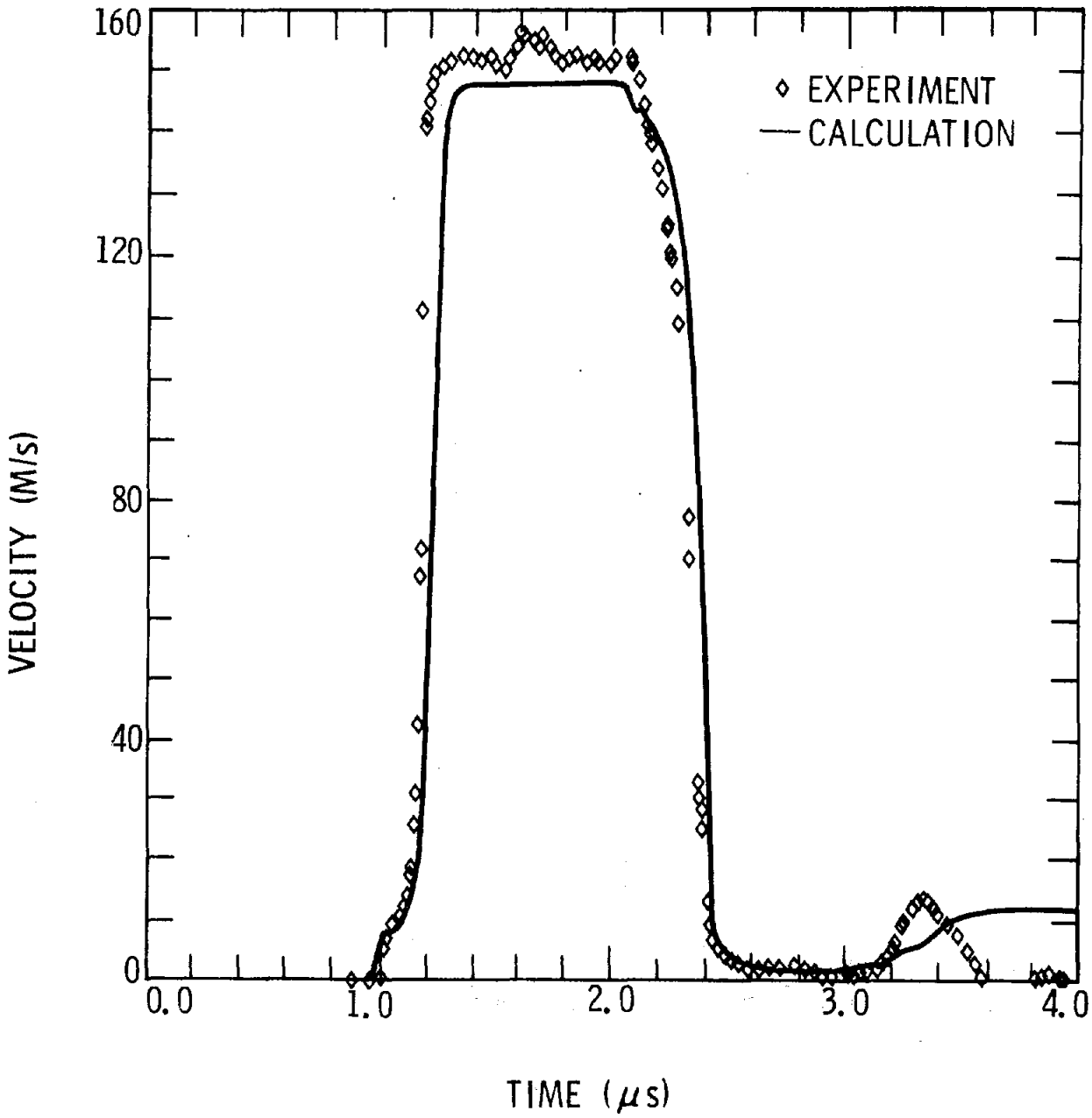

Figure 2. Aluminum/quartz interface velocity history. Dislocation multiplication active.

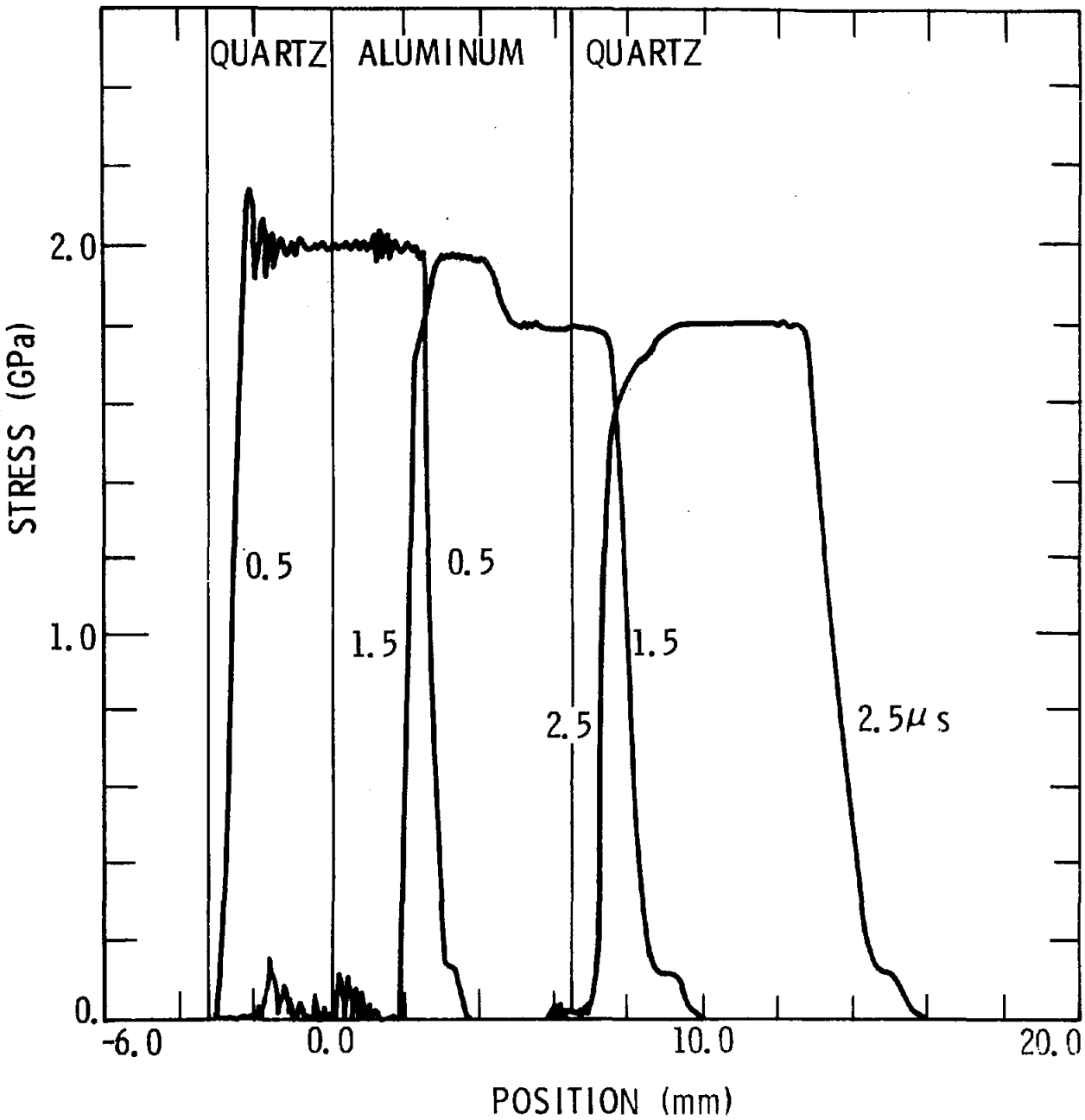

Figure 3. Stress wave profiles at 0.5, 1.5 and 2.5 μs.

$$E_{11} = \sqrt{P_{33}} \left(\frac{1 - \mathcal{D}}{1 - \mathcal{D}_o} \right)^{1/3} .$$

An alternative approach is to consider uniform damage to have been generated with no lateral motion permitted. This results in a residual plastic deformation, $P_{11} = (1 - \mathcal{D}_o)^{1/3}$, if no residual stresses are permitted. Then, from Eq. (4),

$$P_{33} = 1/(1 - \mathcal{D}_o)^{2/3} .$$

Finally, from Eq. (2a), the original distended density is $\rho_o(1 - \mathcal{D}_o)$.

Using this latter method, for an initial $\mathcal{D}_o$ of 0.1, the distended density becomes 2.439 in the aluminum. For the same geometry as considered in example A-2, the target/window velocity history is shown in Figure 4, and the wave profiles at 0.5, 1.5, and 2.5 μs are seen in Figure 5. The minimum stress for collapse, σ_G, is 0.3 GPa, so there is a 0.3 GPa wave travelling through the predamaged material unimpeded.

At the crest of the wave at 1 μs, the temperature has risen from 300°K to 350°K as compared to 317°K in case A-2. The distended material is absorbing much energy as it crushes; these results are consistent with what has been shown using the P-α model for distended materials [e.g., Ref. 6]. It must be emphasized that this example is not intended to model specifically a distended aluminum medium; the parameters employed are strictly for the purpose of illustrating an additional possible interpretation of the present damage model.

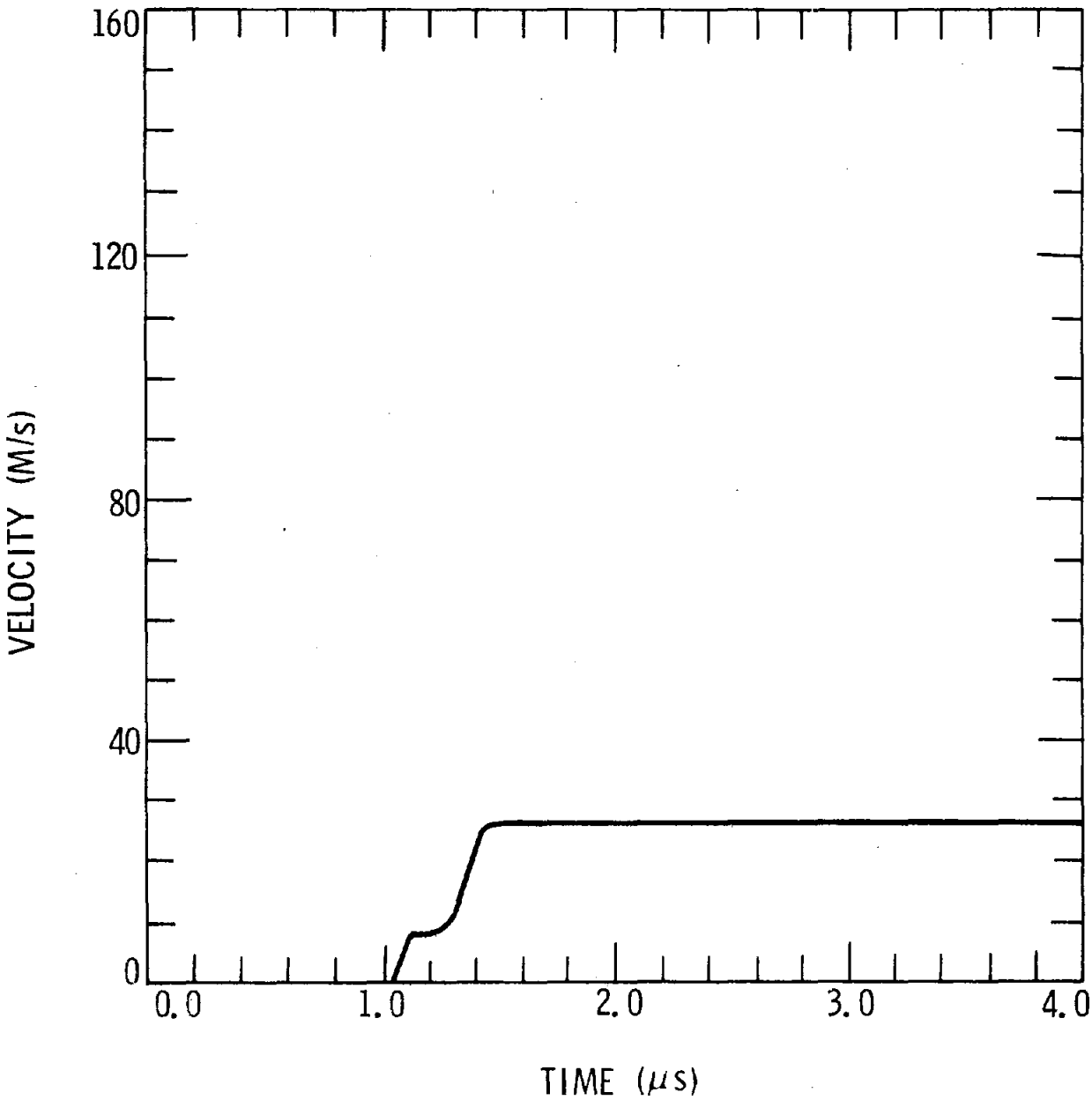

Figure 4. Aluminum/quartz interface velocity history for 10% porous aluminum.

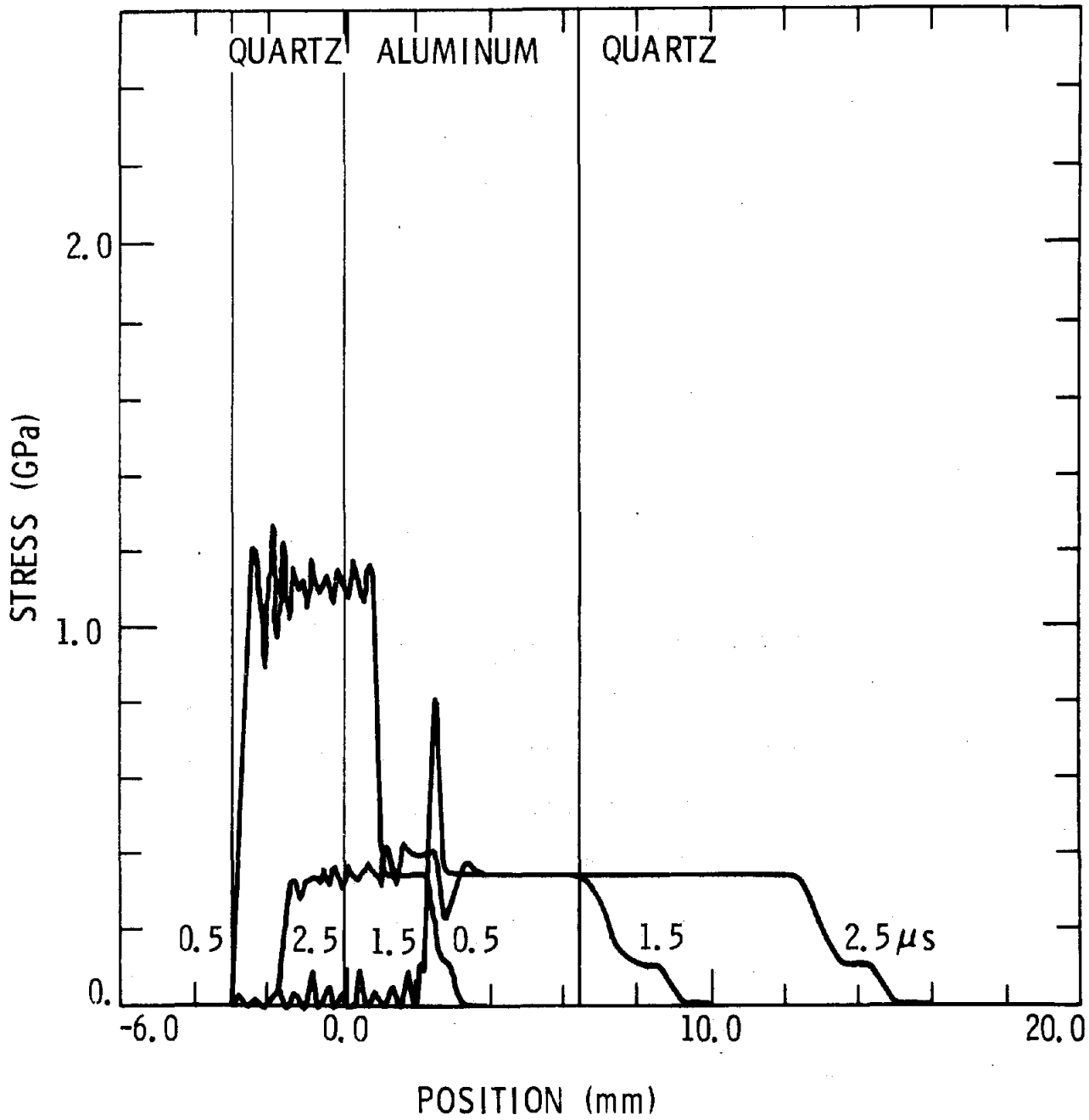

Figure 5. Stress wave profiles for 10% porous aluminum.

B. Fused Quartz Flyer/Aluminum Target

Case B-1.

Using the parameters from Table 2, Appendix D, for the aluminum, but with the dislocation multiplication mechanism turned off ($A^* = -1$), and the damage model suppressed ($C_n = -1$), the aluminum may experience tension, with no resultant spallation. The back surface velocity history is seen in Figure 6, and the stress history at the plane where spallation could have occurred is presented in Figure 7.

Case B-2.

If case B-1 is now expanded to permit damage to occur, we observe dramatic alterations in the rear surface velocity history, Figure 8, and the stress history at the plane of maximum damage, Figure 9. Figure 8 shows some recovery with the expected ringing. The damaged region is now "translucent" to stress waves. The stress wave at the damage plane, Figure 9, shows how the stress relaxes as the damage begins to accumulate and change the material properties of that region. A sequence of wave profiles showing this effect is depicted in Figure 10. The final damage profile is given in Figure 11. While there is a concentrated region of damage that could be called a spall plane, the damage is clearly not limited to a single plane.

Case B-3.

By a process of trial and error, a new set of damage parameters were determined that provide a better fit of the back surface velocity history. These damage parameters are given in Appendix D, Table 3. One immediately apparent aspect is that for some lower impact velocity, the nucleation

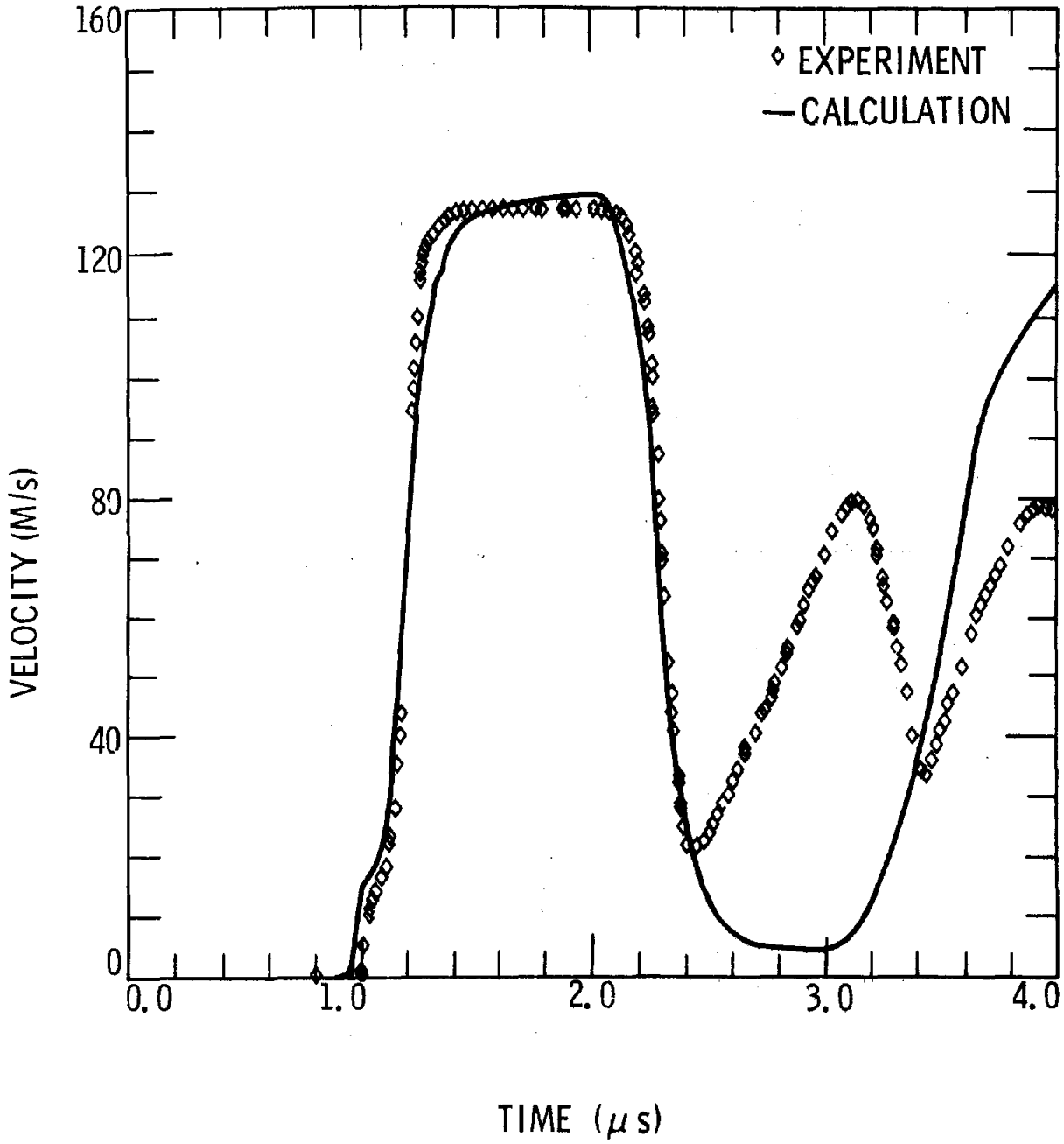

Figure 6. Back surface velocity history for suppressed damage and suppressed dislocation multiplication.

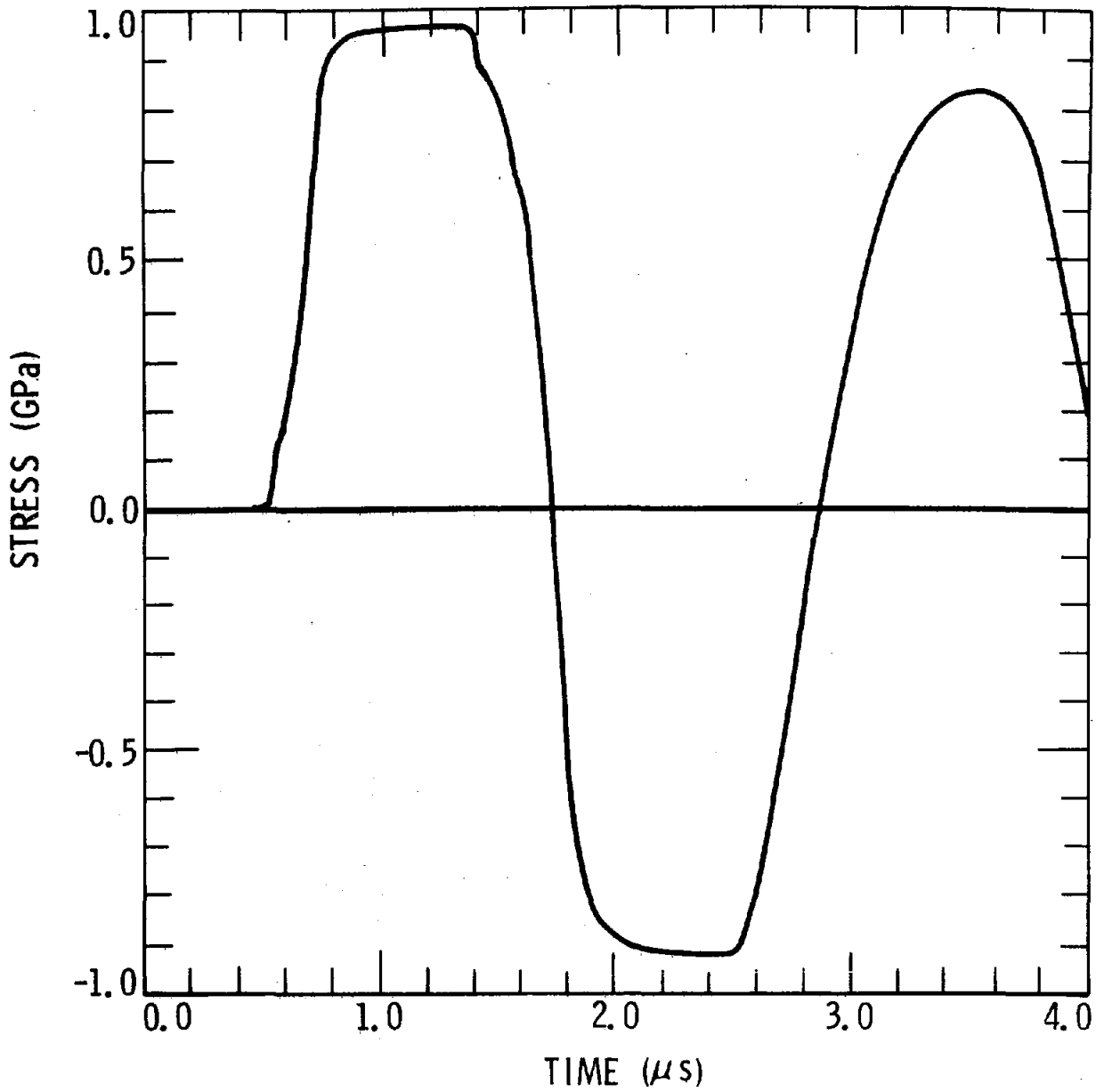

Figure 7. Stress history at plane of expected spall with damage and dislocation multiplication suppressed.

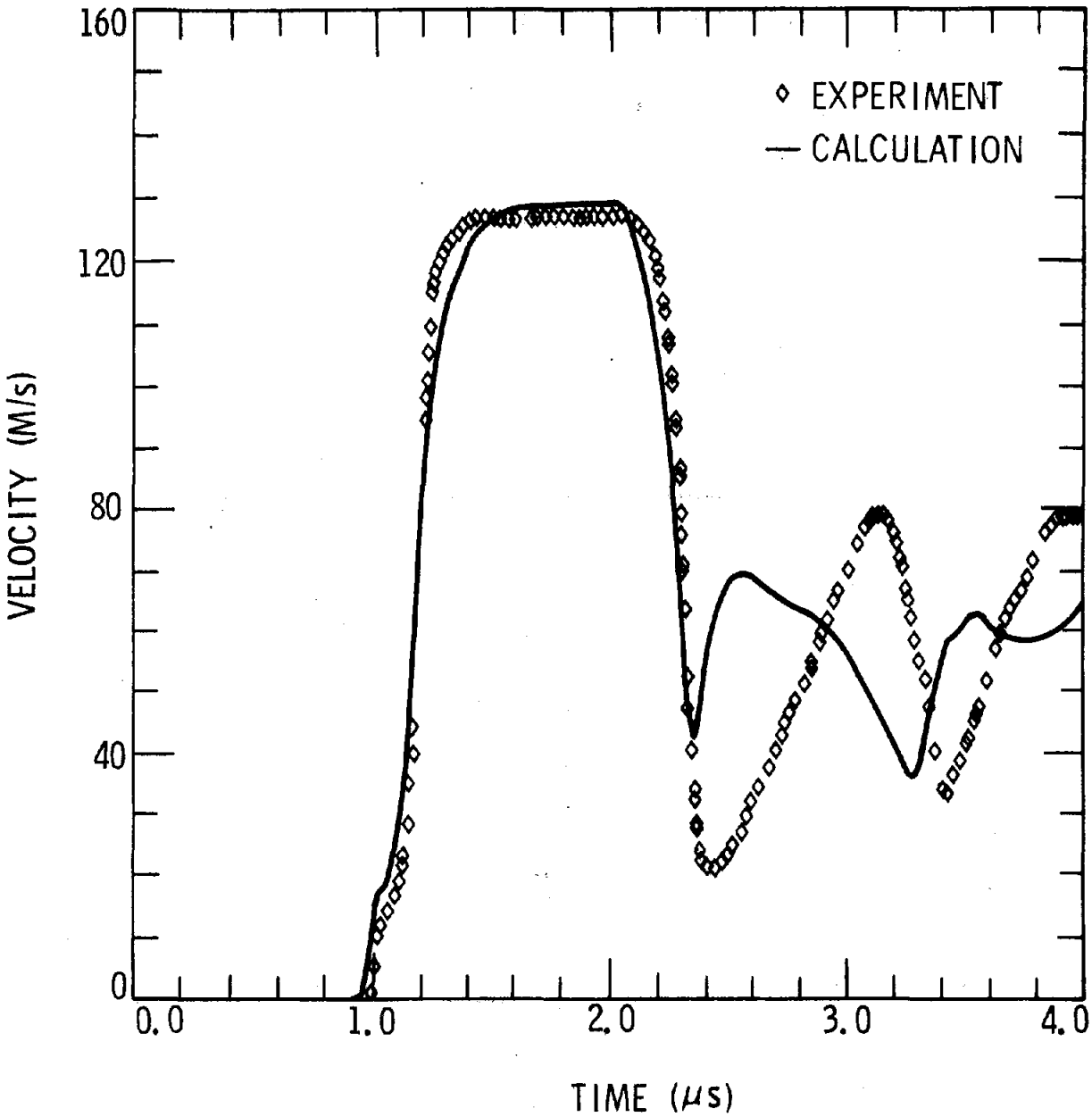

Figure 8. Back surface velocity history with damage forming and dislocation multiplication suppressed. Damage data, Appendix D, Table 2.

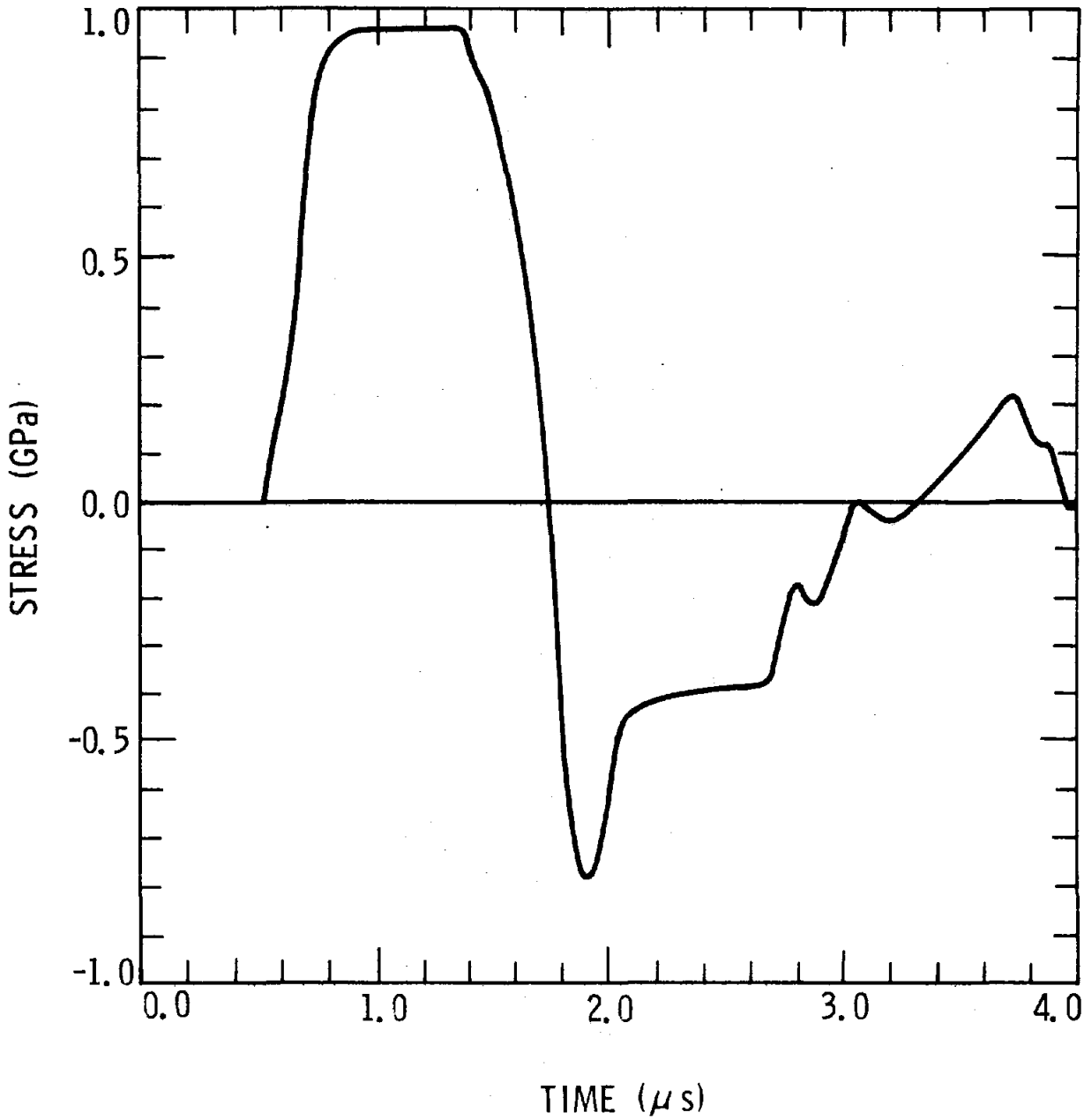

Figure 9. Stress history at plane of maximum damage; dislocation multiplication suppressed. Damage data, Appendix D, Table 2.

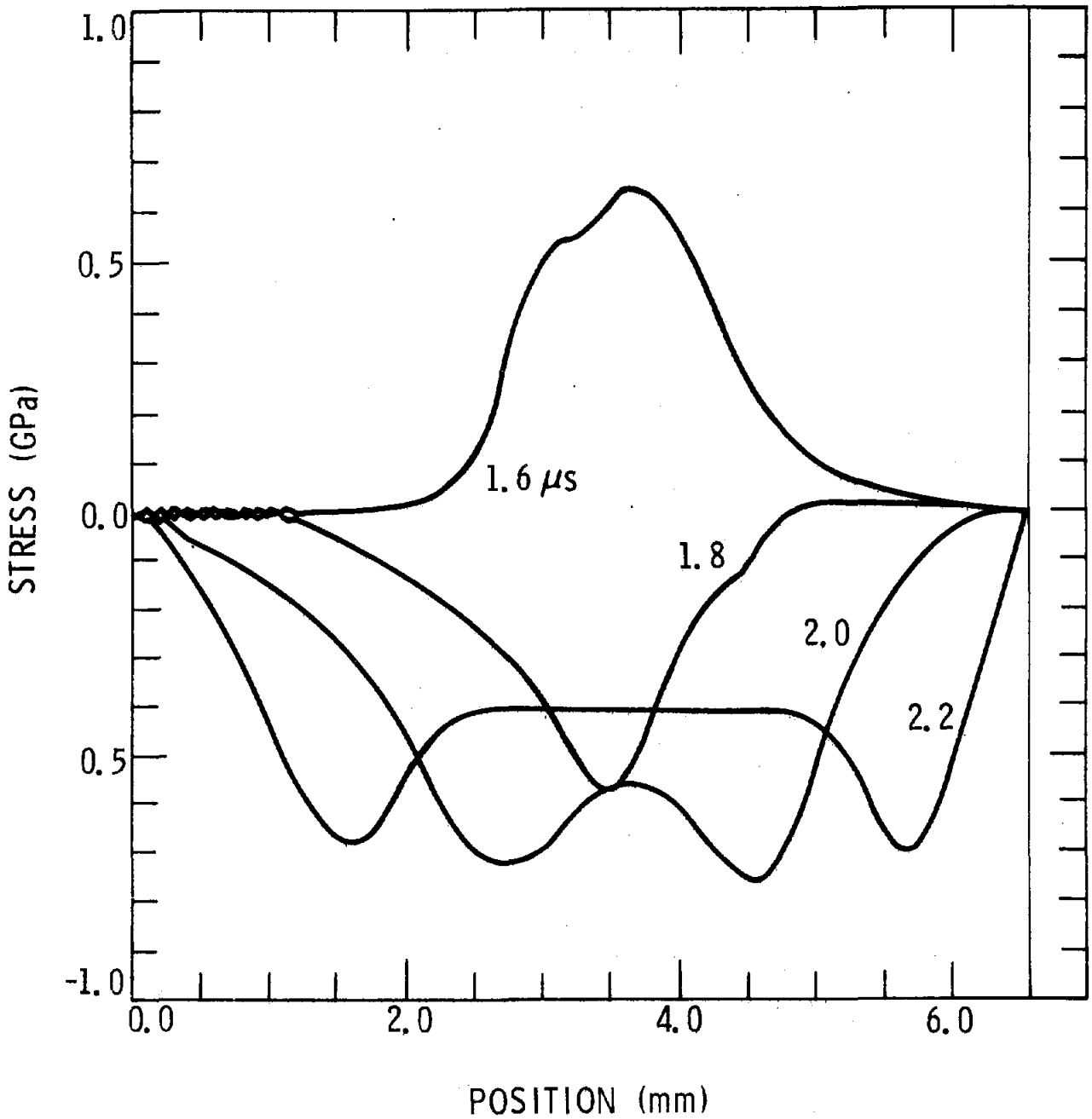

Figure 10. Stress wave profiles in aluminum at 1.6, 1.8, 2.0 and 2.2 μs. Damage data, Appendix D, Table 2.

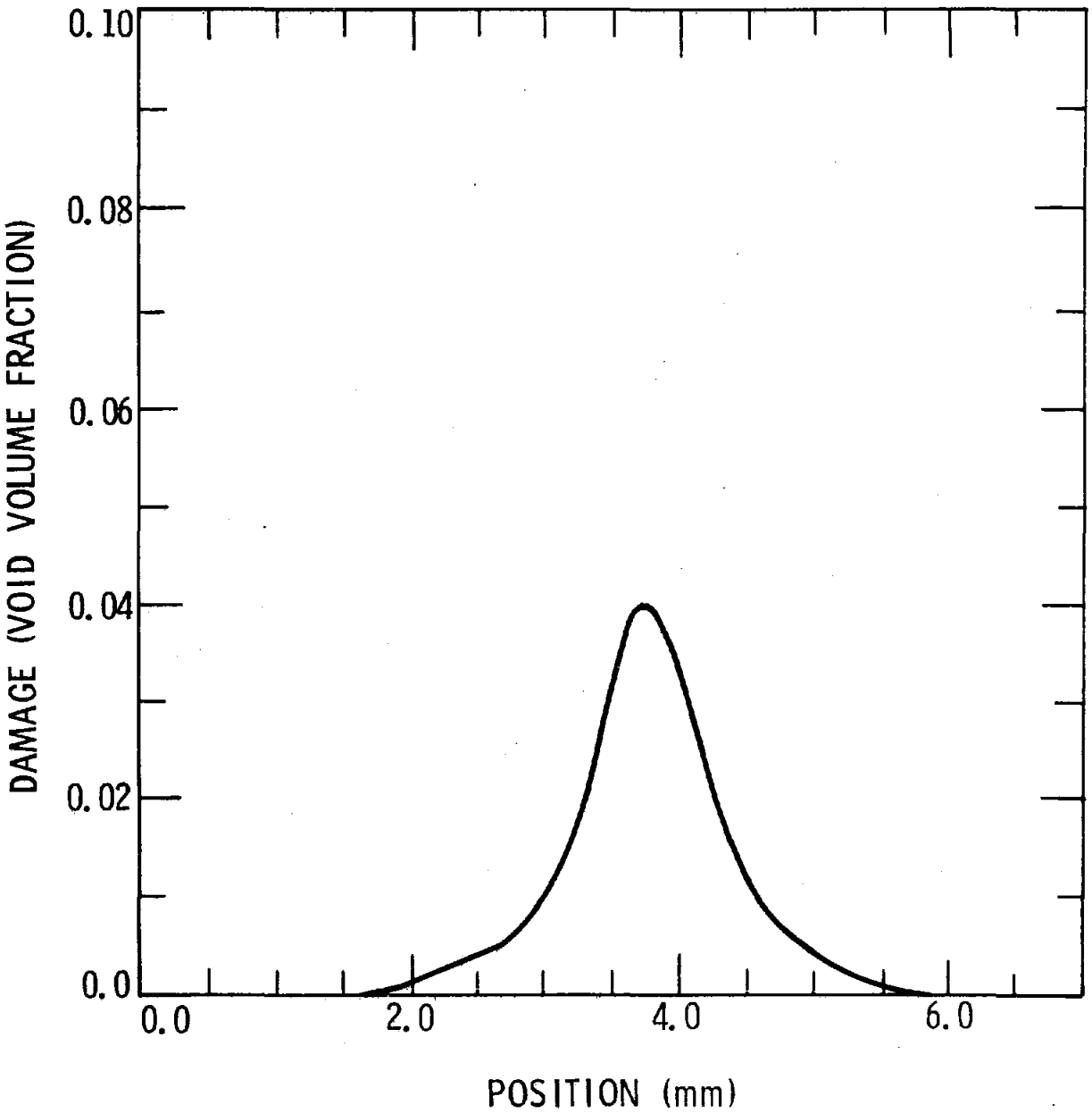

Figure 11. Final damage distribution. Damage data, Appendix D, Table 2.

threshold, σ_n, will not be exceeded and no damage will develop. If, in fact, σ_n is truly a physical property, then it should be possible to isolate it in a series of experiments with a range of impact velocities that indicate when some void formation becomes evident.

Figure 12 illustrates the back surface velocity history resulting from these new damage parameters. Observe specifically that the first minimum has been pulled down to a more appropriate position--this was accomplished primarily by increasing σ_n, to retard the initiation of void formation. The decreased slope of the recovery is attributable to decreasing the rate of growth, governed primarily by C_G. Figure 13 is a plot of the stress history on the plane of maximum damage. Comparison with Figure 9 shows major changes in the stress relaxation caused by the damage growth as governed by the new damage parameters. Figure 14 shows the final damage distribution. It is somewhat more narrow than before (Figure 11). Figure 15 shows the spatial distribution of the void number density, n, and it is seen that a substantial number of voids have been nucleated that did not grow to significant damage levels.

Case B-4.

The dislocation multiplication mechanism is now made operable for the purpose of demonstrating the effects of the plasticity model on the damage behavior experienced by the solid. The damage parameters of case B-3 are retained, and A^* is set back to $1(10^{-4})$ to activate the dislocation mechanism. Figure 16 shows the back surface velocity history. The loading and unloading behavior is clearly more satisfactory, and the wave arrival times are in general more nearly coincident with the experimental record. The more precisely defined wave fronts generate a sharper tensile

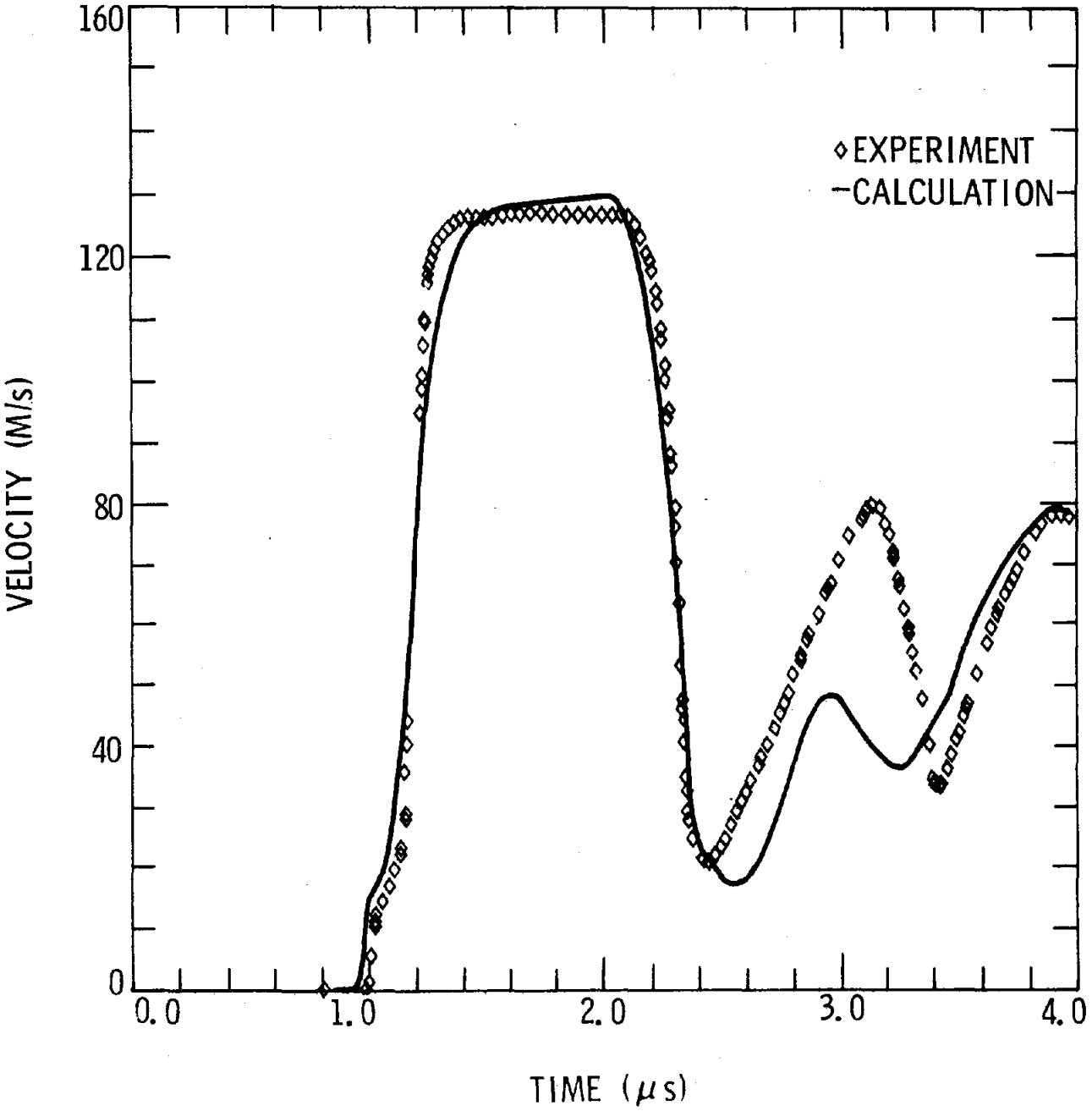

Figure 12. Back surface velocity history with dislocation multiplication suppressed. Damage data, Appendix D, Table 3.

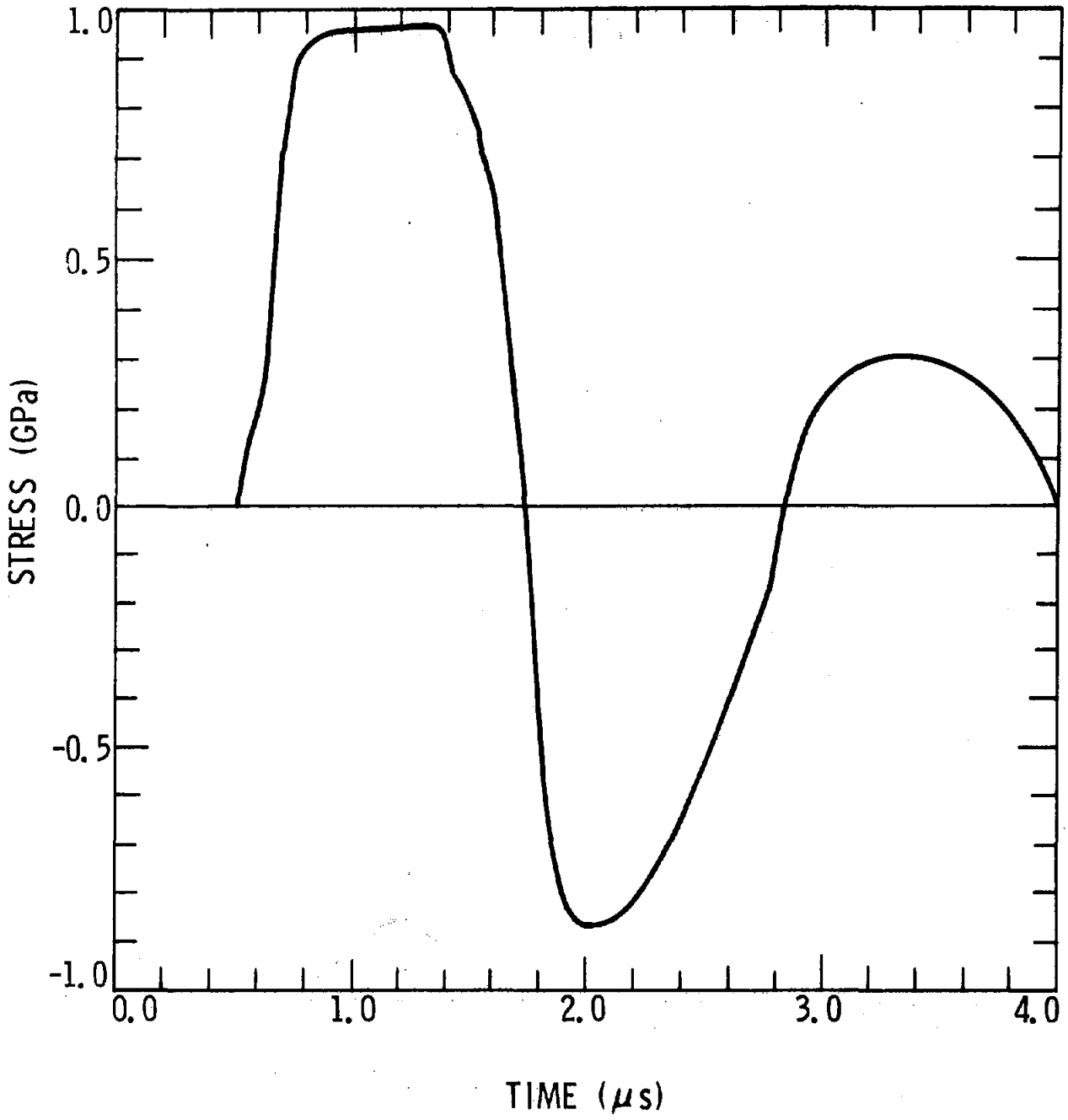

Figure 13. Stress history at plane of maximum damage. Dislocation multiplication suppressed. Damage data, Appendix D, Table 3.

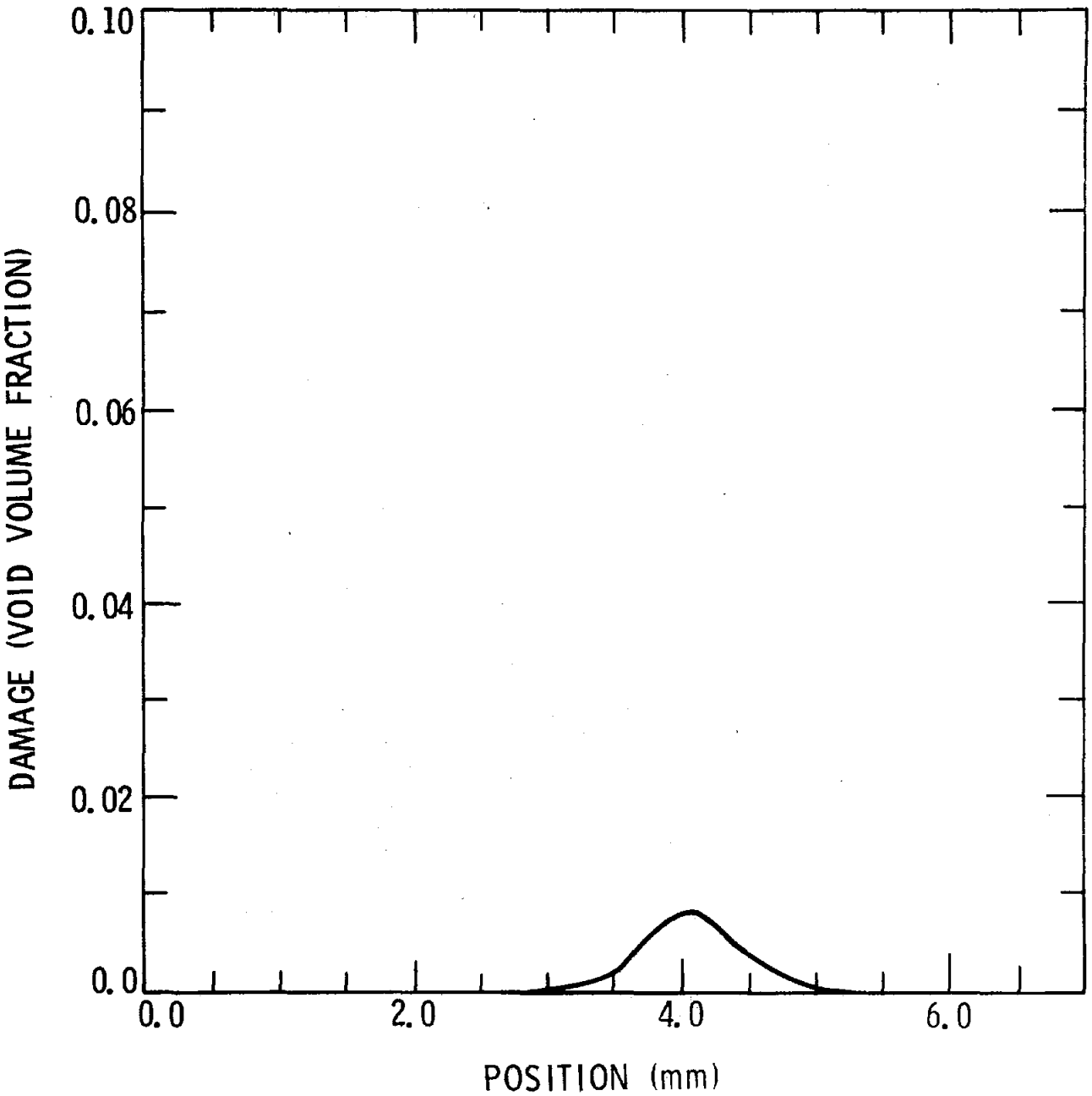

Figure 14. Final damage distribution. Dislocation multiplication suppressed. Damage data, Appendix D, Table 3.

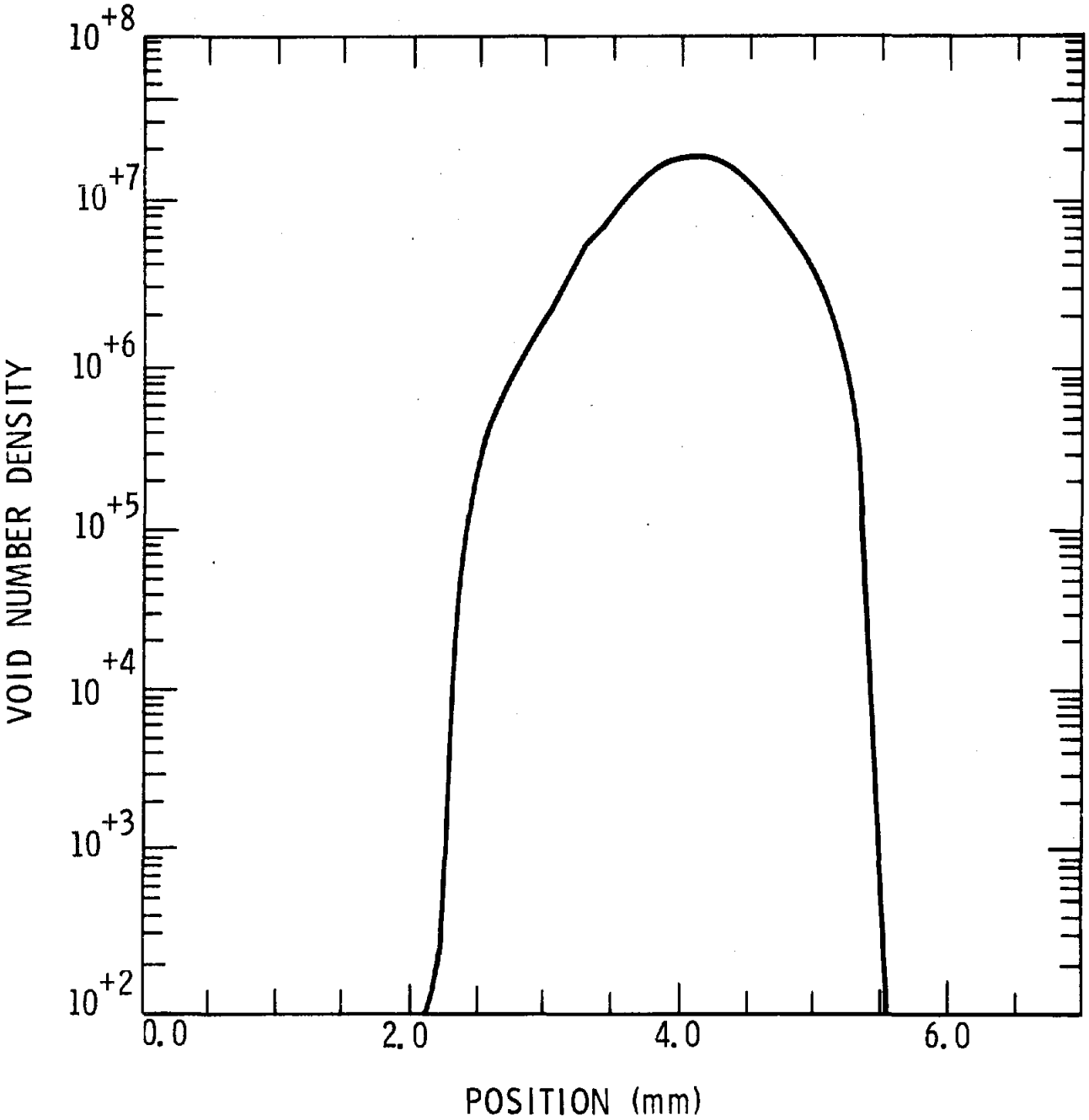

Figure 15. Final void number density. Damage data, Appendix D, Table 3.

pulse which in turn significantly alters the damage growth and pulse decay. This is shown by a stress history at the plane of maximum damage, Figure 17. The resulting damage (Figure 18) is also greater than before, but with a little more spread than seen in Figure 14.

The damage growth history at the plane of maximum damage is seen in Figure 19, indicating a period of void collapse or recoverable damage. Information based only on post-mortem studies would not be expected to reveal such behavior; there is no a priori reason to exclude void collapse during the course of the wave-damage interactions.

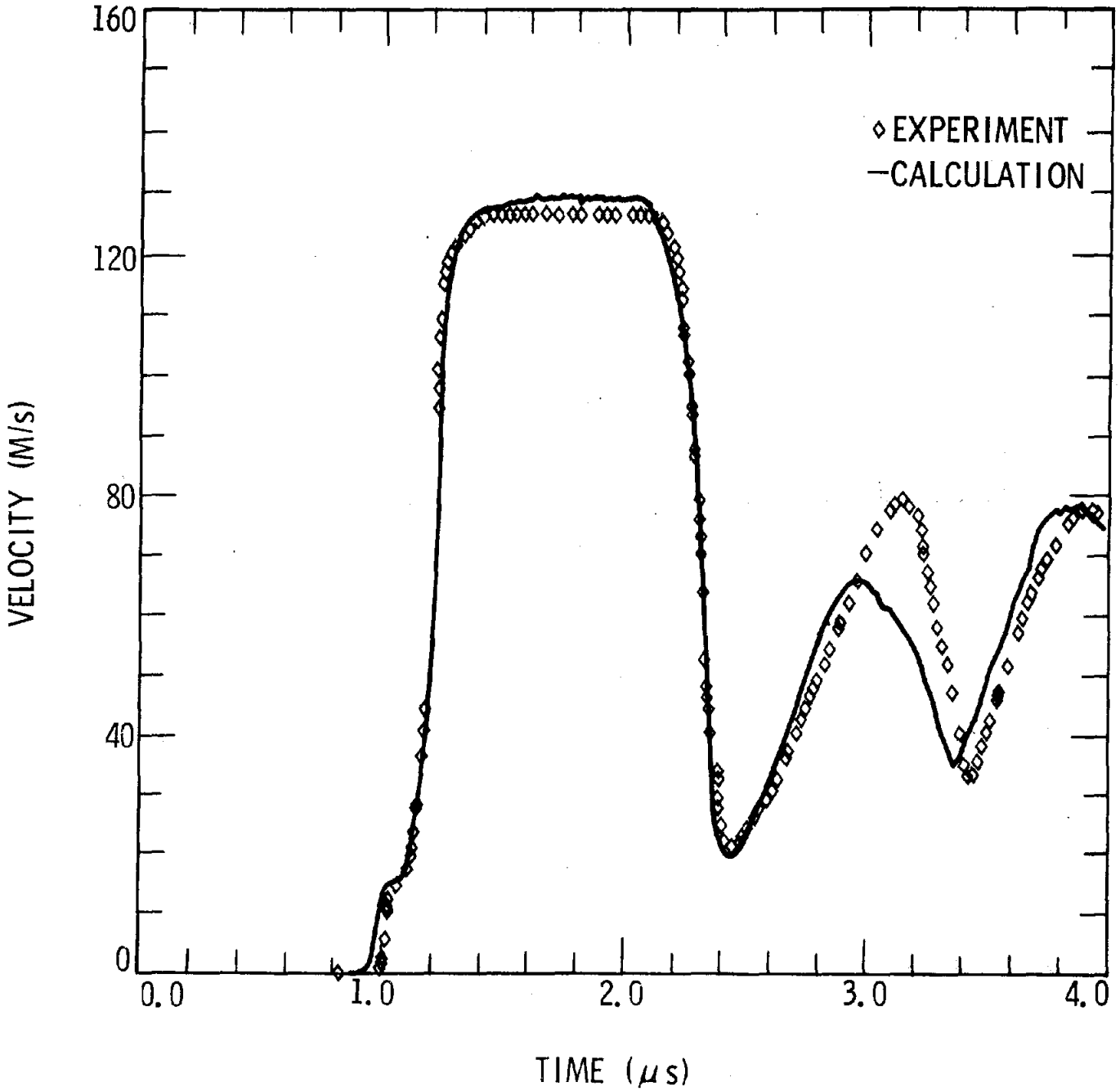

Figure 16. Back surface velocity history. Dislocation multiplication active. Damage data, Appendix D, Table 3.

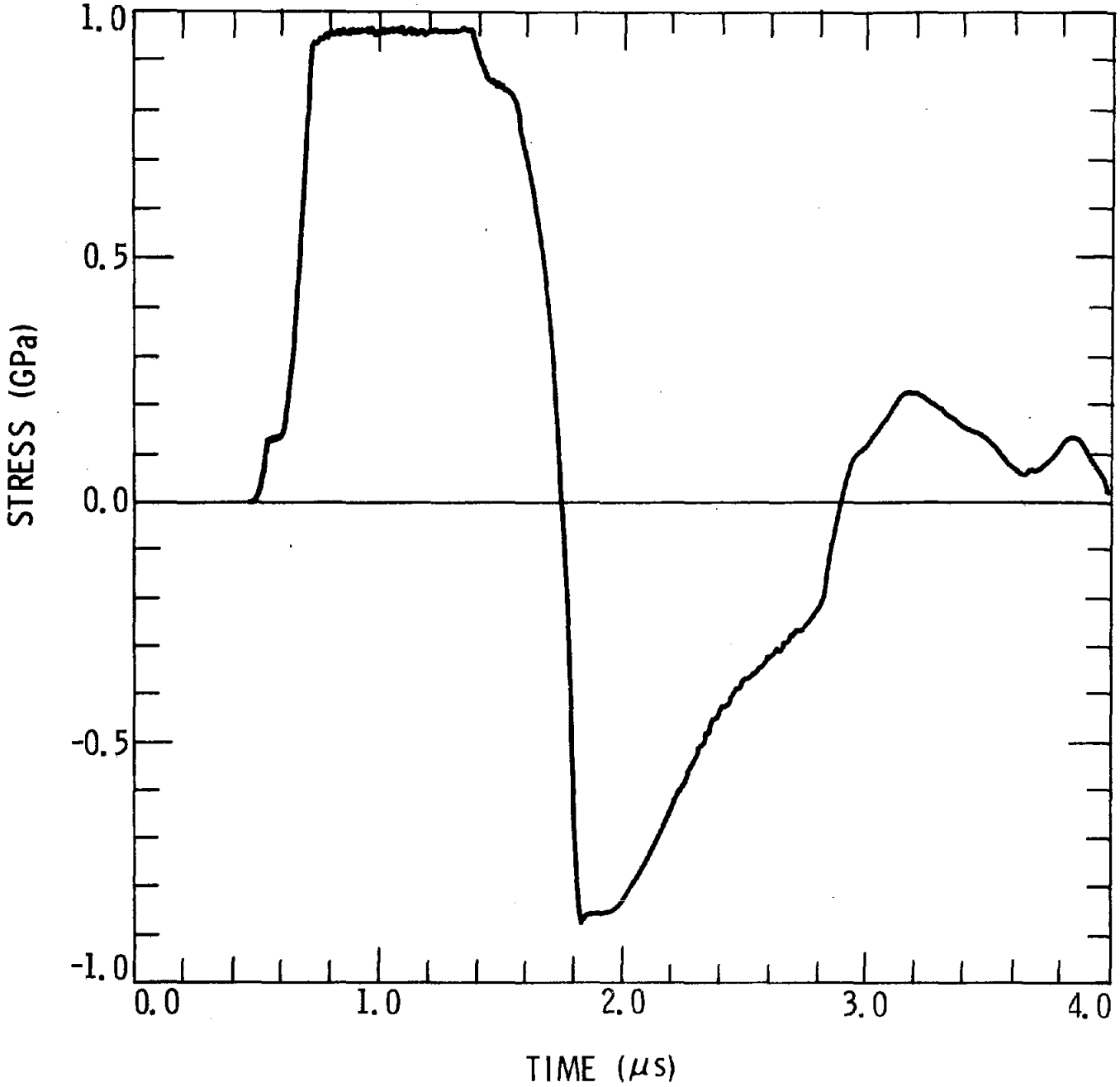

Figure 17. Stress history at plane of maximum damage.
Damage data, Appendix D, Table 3.

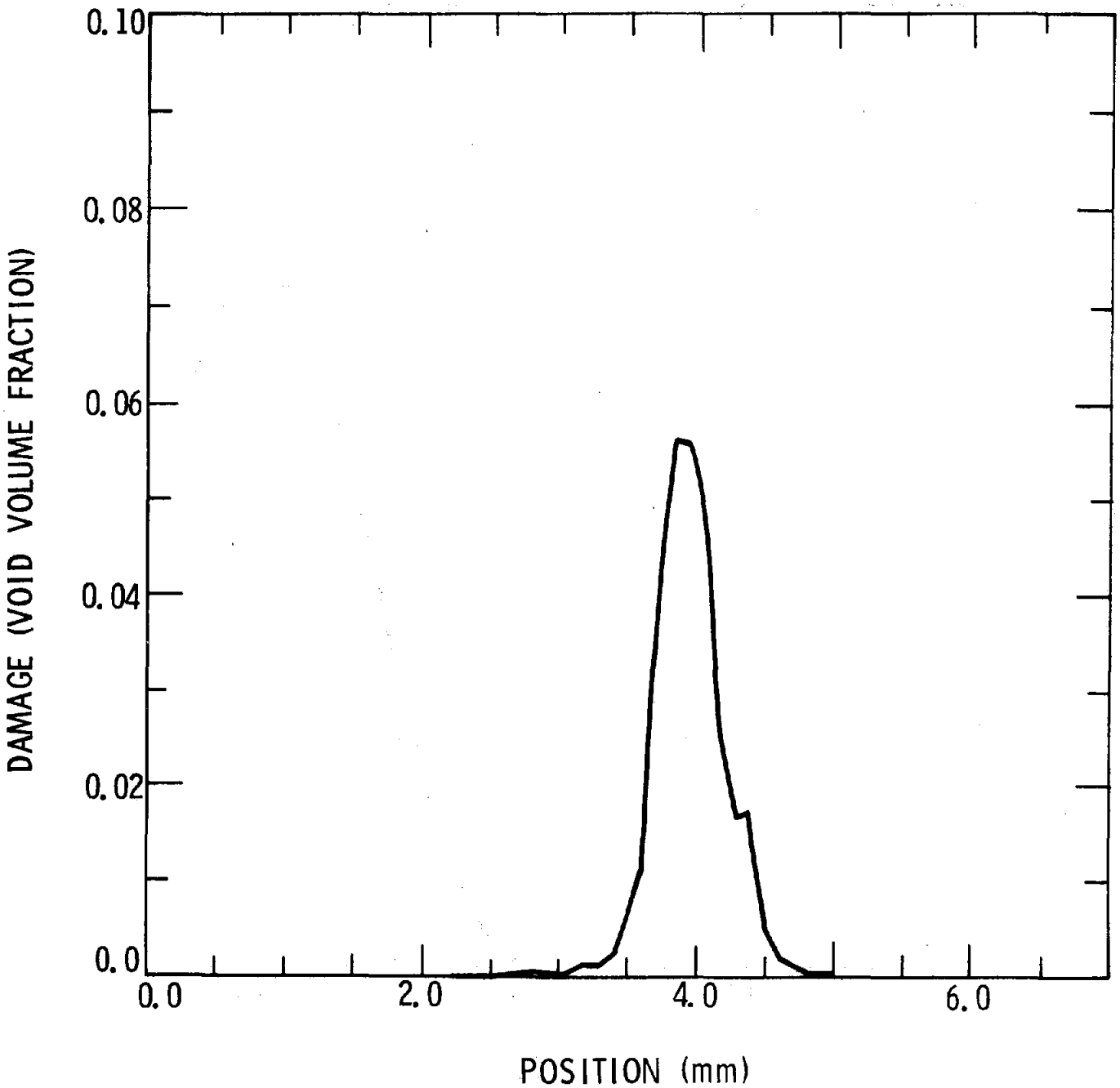

Figure 18. Final damage distribution in aluminum.
Damage data, Appendix D, Table 3.

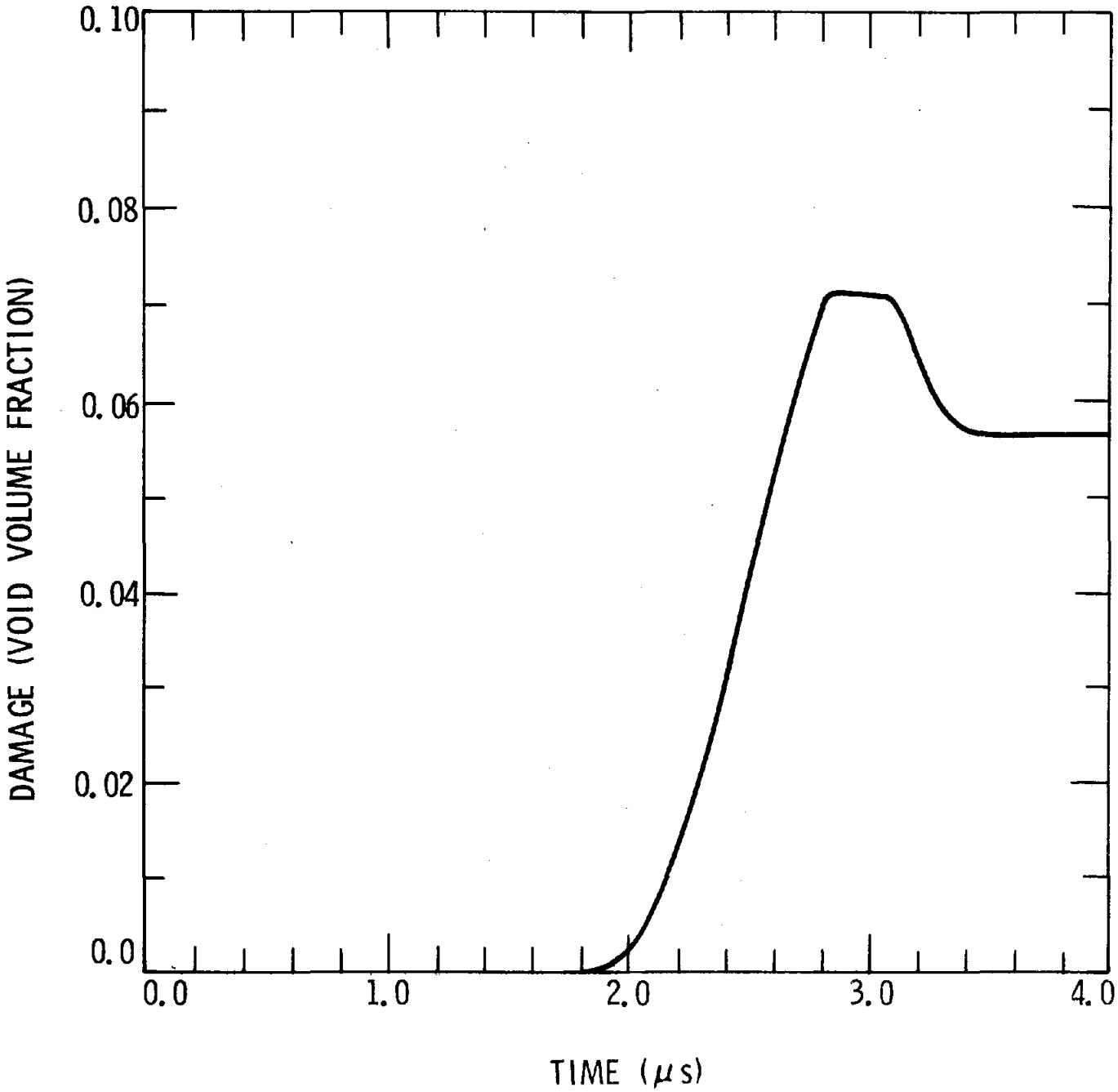

Figure 19. Damage accumulation history at plane of maximum final damage. Damage data, Appendix D, Table 3.

C. Fused Quartz Flyer/Aluminum Target

This coarsely zoned problem is computed using elastic-viscoplastic-damage parameters identical to those of case B-4. Despite the coarse zoning, the back surface velocity history, Figure 20, retains the major aspects of behavior, but the final damage levels, Figure 21, are about 40% lower than for the more finely resolved case.

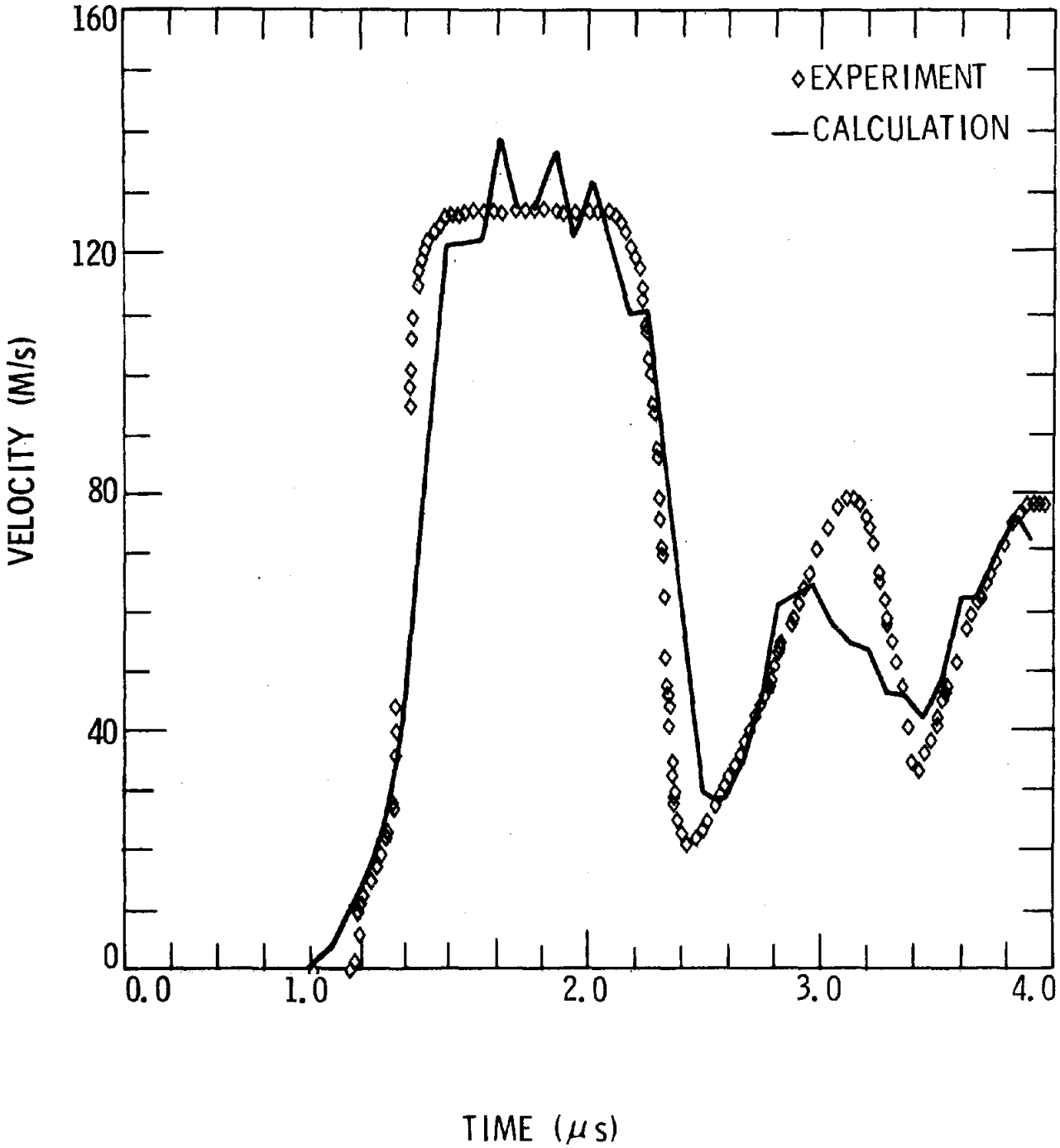

Figure 20. Results of coarse zoning on back surface velocity history. Damage data, Appendix D, Table 3.

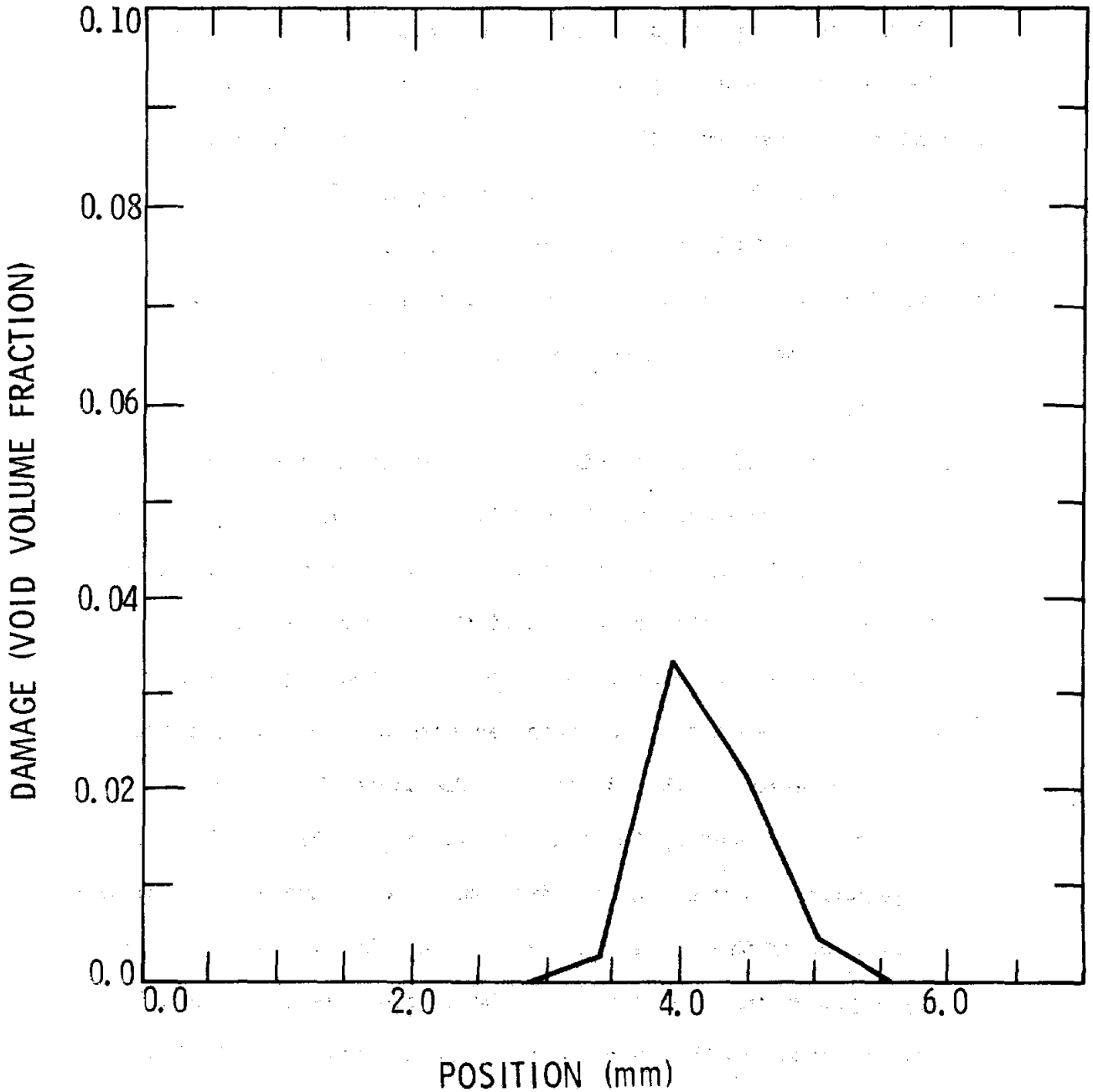

Figure 21. Final damage distribution, coarse zoning.
Damage data, Appendix D, Table 3.

VI. CONCLUSIONS

Although this report is primarily intended to illustrate the method of solution of the governing equations for an elastic-viscoplastic-damage model within the wavecode, WONDY, several example calculations have been included to demonstrate the flexibility of the model. The integrator STEP1 has proved efficient in the task of numerically integrating the differential equations within the confines of the wavecode, and is expected to be a viable method of solution of other model equations requiring similar treatment.

The examples included in this report form an isolated sample of material behavior predicted by the model. The predamage in material is expected to be an integral aspect of rock failure models, where instead of voids, randomly oriented cracks exist that may close prior to growing in other directions. Of particular interest is the high degree of coupling between the elastic-plastic and damage aspects of the model, having observed in the examples that details of the damage behavior are significantly influenced by the elastic-plastic modeling. This implies that the parameters for a constitutive damage model are not independent of the remainder of the model, and are even coupled to the artificial viscosity employed in a wavecode. In the present case, the artificial viscosity was tuned to the resolution of the loading and unloading behavior of the aluminum independent of the damage occurrence, and then the damage parameters adjusted. Although it is much less expensive to run coarsely zoned problems, the lack of damage resolution limits the useful information to come from these runs. A lower limit of resolution needs to be determined above which damage levels are not affected by the resolution.

Finally, it is clear that damage parameters may be at least in part assessed from back surface velocity histories, these histories being a very stringent test of the capabilities and correctness of the damage modeling.

Acknowledgments

The authors express their appreciation to R. J. Lawrence for his advice on fitting this constitutive model into WONDY, to M. K. Gordon for her suggestions that led to the efficient employment of the integrator, STEP1, within the wavecode, and to L. W. Davison for his overall encouragement and guidance in this endeavor.

References

1. Davison, L., Stevens, A. L., and Kipp, M. E., "Spall Damage in Ductile Metals," to be published.
2. Lawrence, R. J. and Mason, D. S., "WONDY IV - A Computer Program for One-Dimensional Wave Propagation with Rezoning," Sandia Laboratories Report, SC-RR-71-0284.
3. Shampine, L. F. and Gordon, M. K., "Computer Solution of Ordinary Differential Equations: The Initial Value Problem," Freeman (1974).
4. Barker, L. M. and Hollenbach, R. E., "Shock-Wave Studies of PMMA, Fused Silica, and Sapphire," J. A. P., Vol. 41, No. 10, pp. 4208-4226, 1970.
5. Seaman, L., Barbee, T. W., Jr., and Curran, D. R., U. S. Air Force Weapons Laboratory Report AFWL-TR-71-156.
6. Herrmann, W., "Constitutive Equation for the Dynamic Compaction of Ductile Porous Materials," Sandia Laboratories Report, SC-R-69-1185.

Appendix A

The WONDY storage arrangements are listed below; WONDY requires 17 variables designated to run with this model.

DATB (2)	STORE (J+12)	n	Number of voids/unit volume
DATB (3)	STORE (J+13)	ϑ	Damage, void volume fraction
DATB (4)	STORE (J+14)	$D_{(T)}$	Dislocation density
DATB (5)	STORE (J+15)	$f_{(m)}$	Mobile fraction of dislocations
DATB (6)	STORE (J+16)	P_{33}	Longitudinal plastic deformation
DATB (7)	STORE (J+17)	θ	Absolute (Kelvin) temperature
	STORE (J+2)	ε	Internal energy

The parameters for the model are stored in CES(N, PLATE) in WONDY, and are on data cards 15-19 in input sequence.

N	Card 15
1	ρ_R, reference density
2	C_d, longitudinal sound speed
3	μ_o, shear modulus
4	ν_o, Poisson's ratio
5	κ_o, bulk modulus (calculated internally)
6	$15(1 - \nu_o)/(7 - 5\nu_o)$ μ coefficient (calculated internally)
7	$3(1 - \nu_o)/2(1 - 2\nu_o)$ κ coefficient (calculated internally)

N	Card 16
8	B, Burgers' vector
9	m, exponent in Eq. (16)
10	τ^*, shear coefficient

11 $C_S = \sqrt{\mu_o/\rho_R}$, shear velocity (calculated internally)

12 $\tau_{(A_o)}$, initial backstress

13 γ_o, yield constant

14 $1/n$, yield exponent

N	Card 17
15	DSTZ, initial dislocation density
16	A^*, $\dot{D}_{(T)}$ coefficient (if < 0, sets $\dot{D}_{(T)} \equiv 0$)
17	$D^*_{(T)}$, saturation dislocation density
18	FSMZ, initial fraction of mobile dislocations
19	B^*, $\dot{f}_{(m)}$ coefficient (if < 0, sets $\dot{f}_{(m)} \equiv 0$)
20	$f^*_{(m)}$, saturation fraction of mobile dislocations
21	(Not used)

N	Card 18
22	C_η, nucleation parameter (if < 0, $\dot{\eta} \equiv \dot{\vartheta} \equiv 0$)
23	σ_1, nucleation parameter
24	σ_η, nucleation threshold
25	υ_o, initial void volume
26	C_G, growth parameter
27	σ_G, growth threshold
28	(Not used)

N	Card 19
29	EPS, STEP1 error tolerance
30	θ_R, reference temperature (if < 1, $\dot{\theta} \equiv 0$)
31	α, coefficient of thermal expansion
32	$\underset{\sim}{C_t}$, specific heat at constant stress

33 (Not used)

34 (Not used)

35 (Not used)

APPENDIX B

EQUATION OF STATE ROUTINE, STAT5 AND F(T,Y,YP), IN WONDY IV

```
      SUBROUTINE STAT5
C     WONDY IV
      COMMON STORE(19870),NEXT(1805),DUM(9025)
      COMMON /CONST/ ADDATA(100), B1, B2, CES(42,20), EXIT, IALPHA,
     1   IDUMP, J, JA, KM(3), KT1, L, LMAX, LOL, LOR, LPHA,
     2   NOMESH(20), NONE, NOP, NTWO, NVAR, PLATE, PRINTE, PRINTL,
     3   PRINTN, STATE(20), SUMQE, TDEP, WL, WR, W4020, XZERO
      COMMON /NAMES/ C, CN, E, EN, M, P, PA, PN, Q, QA, QN, R, RA, RN,
     1   S, SA, SN, U, UA, UB, UBN, UN, X, XA, XB, XBN, XN, Z, ZA, ZN
      COMMON /RETAIN/ N, T, DELT(5), ETOT, HTOT, ITABLE(50), TABLE(2,50)
     1  , PFRACT(1805), QFRACT(1805), LACT
      COMMON /JMSO/ DATB(100), DELRHO, DELXJ, JONE, NEWPLAT, RHODOT
      COMMON /WJSD/ DEP, FCONST(20), FCONSTI(20), FCRIT(20), FCRITI(20),
     1   JTAPE, LDUMP, NSTART, SIGACT, SIGMAF(20), SIGMAIF(20),
     2   SIGMAO(20), SIGMAOI(20), SIGSEP
      DIMENSION Y(7),WT(7),PHI(7,16),PP(7),YP(7),PSI(12),ALPHA(12),
     1 BETA(12),SIG(13),V(12),W(12),G(13),YOUT(7),YPOUT(7)
      COMMON /TIMESF/ DELTIM,TZERO,TEND
      TYPE INTEGER PLATE, W4020
      TYPE LOGICAL START, CRASH, PHASE1, NORND, STIFF
      EXTERNAL F
C
C     WONDY   STATE 5
C     REFERENCES
C     DAVISON, STEVENS, KIPP - SPALL DAMAGE IN DUCTILE METALS (1976)
C     KIPP, STEVENS - SANDIA REPORT  SAND-76-0061
C     METHOD OF SOLUTION OF COUPLED FIRST O-DE- O-D-NA-O D-FFERENT-AL
C     EQUATIONS  -  STEP, INTRP
C     STEP  IS A VARIABLE ORDER, VARIABLE STEP ADAMS METHOD INTEGRATOR
C     INTRP  INTERPOLATES TO FINAL TIME
C     REFERENCE  -  L F SHAMPINE AND M K GORDON, COMPUTER SOLUTION OF
C     ORDINARY DIFFERENTIAL EQUATIONS-THE INITIAL VALUE PROBLEM
C     FREEMAN (1974)
C     NUMBER OF VARIABLES REQUIRED IS 17
C     NOTATION
C     DATB(2)=VNUM  NUMBER OF VOIDS/UNIT VOLUME
C     DATB(3)=DMG   DAMAGE   VOID VOLUME FRACTION
C     DATB(4)=DST   DISLOCATION DENSITY
C     DATB(5)=FSM   FRACTION OF MOBILE DISLOCATIONS
C     DATB(6)=P33   LONGITUDINAL PLASTIC DEFORMATION
C     DATB(7)=THETA TEMPERATURE IN KELVIN DEGREES
      DELTIM=DELT(1)
      TZERO=T-DELTIM
      TEND=T
C
C     INITIALIZATION OF PARAMETERS FOR STEP
      H=DELTIM
      DO 5 KKK=1,6
```

```
    5   Y(KKK)=DATB(KKK+1)
        Y(7)=E
        TPRES=TZERO
        NEQN=7
        START=.TRUE.
        STIFF=.FALSE.
        KLE4=0
        KSTF=0
C
C       ERROR INFORMATION
        EPS=CES(29,PLATE)
   10   WT(1)=Y(1)/EPS/EPS
        IF(Y(1).LE.EPS)WT(1)=1.0/EPS/EPS
        WT(2)=Y(2)
        IF(Y(2).LE.EPS)WT(2)=EPS
        WT(3)=Y(3)
        WT(4)=Y(4)
        IF(Y(4).LE.EPS)WT(4)=EPS
        WT(5)=Y(5)
        WT(6)=Y(6)
        IF(Y(6).LE.EPS)WT(6)=EPS
        WT(7)=Y(7)/EPS/EPS
        IF(Y(7).LE.EPS)WT(7)=1.0/EPS/EPS
   15   CALL STEP1(F,NEQN,Y,TPRES,H,EPS,WT,START,HOLD,K,KOLD,CRASH,PHI,PP,
       1 YP,PSI,ALPHA,BETA,SIG,V,W,G,PHASE1,NS,NORND)
        IF(CRASH)GO TO 15
C
C       STIFFNESS CHECK
        KLE4=KLE4+1
        KSTF=KSTF+1
        IF(KOLD.GT.4)KLE4=0
        IF(KLE4.GE.50)STIFF=.TRUE.
        IF(KSTF.LT.500)GO TO 20
        IF(STIFF)PRINT 25,TPRES,N,L
        KLE4=0
        STIFF=.FALSE.
   25   FORMAT(/,*      EQUATIONS ARE STIFF, AT TIME*,E12.4,*   CYCLE=*,I5,
       1*   ZONE=*,I5)
   20   CONTINUE
        IF(TPRES.GE.T)GO TO 30
        H=AMIN1(H,1.00001*(T-TPRES))
        GO TO 10
   30   CALL INTRP(TPRES,Y,T,YOUT,YPOUT,NEQN,KOLD,PHI,PSI)
        DO 35 KKK=1,6
   35   DATB(KKK+1)=YOUT(KKK)
        EN=YOUT(7)
        SP33=SQRT(DATB(6))
        FRZRH=CES(1,PLATE)/RN
        AMU=CES(3,PLATE)*(1.-CES( 6,PLATE)*DATB(3))
        IF(AMU.LT.0.)AMU=0.
        AKAP=CES(5,PLATE)*(1.-CES( 7,PLATE)*DATB(3))
        IF(AKAP.LT.0.)AKAP=0.
        EM=1./(1.-DATB(3))**0.333333
        E11=SP33/EM
```

```
      E33=FRZRH/EM/DATB(6)
      EPS11=E11-1.
      EPS33=E33-1.
      STHERM=3.*CES(31,PLATE)*AKAP*(DATB(7)-CES(30,PLATE))
      T33=2.*(AKAP-2.*AMU/3.)*EPS11+(AKAP+4.*AMU/3.)*EPS33 - STHERM
      SN=-T33
      TAU=AMU*EM*EM*(EPS33-EPS11)
      ZN=-2.0*TAU
C     ELASTIC SOUND SPEED
      CN=CES(2,PLATE)
      RETURN
C
C
C     CALCULATION OF CONSTANTS FOR EQUATION OF STATE 5
      ENTRY STIN5
C      BULK MODULUS RECALCULATED
      CES(5,PLATE)=2.0*CES(3,PLATE)*(1.+CES(4,PLATE))/3.0/
     1 (1.-2.0*CES(4,PLATE))
C     LONGITUDINAL WAVE VELOCITY RECALCULATED
      CES(2,PLATE)=SQRT((CES(5,PLATE)+4.*CES(3,PLATE)/3.)/CES(1,PLATE))
C     COEFFICIENT IN DAMAGE EQUATION FOR SHEAR MODULUS
      CES( 6,PLATE)=15.0*(1.-CES(4,PLATE))/(7.-5.*CES(4,PLATE))
C     COEFFICIENT IN DAMAGE EQUATION FOR BULK MODULUS
      CES( 7,PLATE)=3.0*(1.-CES(4,PLATE))/2./(1.-2.*CES(4,PLATE))
C     SHEAR WAVE VELOCITY
      CES(11,PLATE)=SQRT(CES(3,PLATE)/CES(1,PLATE))
C     INITIALIZE STORE ARRAY FOR NEW VARIABLES
      DO 40 LA=LOL,LOR
      JA=(LA-1)*NVAR
C     VOID NUMBER DENSITY
      STORE(JA+12)=0.
C     DAMAGE -(VOID VOLUME FRACTION)
      STORE(JA+13)=0.
C     DISLOCATION DENSITY
      STORE(JA+14)=CES(15,PLATE)
C     MOBILE DISLOCATION FRACTION
      STORE(JA+15)=CES(18,PLATE)
C     LONGITUDINAL DEFORMATION GRADIENT - PLASTIC
      STORE(JA+16)=1.0
C     TEMPERATURE
      STORE(JA+17)=CES(30,PLATE)
   40 CONTINUE
      RETURN
      END
```

```
      SUBROUTINE F(T,Y,YP)
      COMMON /CONST/ ADDATA(100), B1, B2, CES(42,20), EXIT, IALPHA,
     1   IDUMP, J, JA, KM(3), KT1, L, LMAX, LOL, LOR, LPHA,
     2   NOMESH(20), NONE, NOP, NTWO, NVAR, PLATE, PRINTE, PRINTL,
     3   PRINTN, STATE(20), SUMQE, TDEP, WL, WR, W4020, XZERO
      COMMON /NAMES/ C, CN, E, EN, M, P, PA, PN, Q, QA, QN, R, RA, RN,
     1   S, SA, SN, U, UA, UB, UBN, UN, X, XA, XB, XBN, XN, Z, ZA, ZN
      COMMON /TIMESF/ DELTIM,TZERO,TEND
      DIMENSION Y(7),YP(7)
      TYPE INTEGER PLATE, W4020
C     CUMULATIVE DERIVATIVE EVALUATIONS CALLED BY STEP
      CES(42,20)=CES(42,20)+1.0
      VNUM=Y(1)
      DMG=Y(2)
      DST=Y(3)
      ESM=Y(4)
      P33=Y(5)
      THETA=Y(6)
      SP33=SQRT(P33)
C
C     LINEAR DENSITY VARIATION FOR TIME INTERVAL
      DENS=((RN-R)*T+R*TEND-RN*TZERO)/DELTIM
      FRZRH=CES(1,PLATE)/DENS
C     LINEAR ARTIFICIAL VISCOSITY VARIATION FOR TIME INTERVAL
      QT=((QN-Q)*T+Q*TEND-QN*TZERO)/DELTIM
C
C     ELASTIC CONSTANTS - DAMAGE EFFECTS
      AMU=CES(3,PLATE)*(1.-CES( 6,PLATE)*DMG)
      IF(AMU.LT.0.)AMU=0.
      AKAP=CES(5,PLATE)*(1.-CES( 7,PLATE)*DMG)
      IF(AKAP.LT.0.)AKAP=0.
C
C     DAMAGE DEFORMATION CONTRIBUTION
      EM=1./(1.-DMG)**0.333333
C
C     ELASTIC DEFORMATIONS
      E11=SP33/EM
      E33=FRZRH/EM/P33
C
C     ELASTIC STRAINS
      EPS11=E11-1.
      EPS33=E33-1.
C
C     THERMAL STRESS CONTRIBUTION
      STHERM=3.*CES(31,PLATE)*AKAP*(THETA -CES(30,PLATE))
C
C     (ELASTIC) STRESSES
      T11=2.*(AKAP+AMU/3.)*EPS11+(AKAP-2.*AMU/3.)*EPS33 - STHERM
      T33=2.*(AKAP-2.*AMU/3.)*EPS11+(AKAP+4.*AMU/3.)*EPS33 - STHERM
C
C     AVERAGE STRESS
      SIG=(2.*T11+T33)/3.
C
C     DAMAGE EQUATIONS
```

```
      IF(CES(22,PLATE).GT.0.0)GO TO 10
      YP(1)=0.0
      YP(2)=0.0
      GO TO 20
   10 CONTINUE
      SNUC=(SIG-CES(24,PLATE)+ABS(SIG-CES(24,PLATE)))/2./CES(23,PLATE)
      SGROW=(2.*SIG+ABS(SIG-CES(27,PLATE))-ABS(SIG+CES(27,PLATE)))/2.
C
C     RATE OF NUCLEATION OF VOIDS
      YP(1)=CES(22,PLATE)*(EXP(SNUC)-1.)
C
C     RATE OF DAMAGE GROWTH
C     NON NORMALISED FORM FOR GROWTH EQUATION CONSTANT  CG
      YP(2)=YP(1)*CES(25,PLATE)*(1.-DMG)*(1.-DMG) + 3.*CES(26,PLATE)*
     1 SGROW*DMG*(1.-DMG)
   20 CONTINUE
C
C     SHEAR STRESS
      TAU=AMU*EM*EM*(EPS33-EPS11)
C     BACK STRESS
      GAM=2.*ABS(ALOG(P33))
      TAUA=CES(12,PLATE)*(1.+(GAM/CES(13,PLATE))**CES(14,PLATE))
C
C     DISLOCATION VELOCITY
      ABTAU=ABS(TAU)
      ES=(ABTAU-TAUA)/CES(10,PLATE)
      VETAU=0.
      Z1=CES(9,PLATE)
      IF(ES.GT.0.)VETAU=CES(11,PLATE)*TAU/ABTAU*(ES**Z1)/(1.+ES**Z1)
C
C     DISLOCATION DENSITY
      YP(3)=0.0
      IF(CES(16,PLATE).GT.0.0) YP(3)=CES(16,PLATE)*(CES(17,PLATE)-DST)*
     1 DST*FSM*ABS(VETAU)
C
C     FRACTION OF MOBILE DISLOCATIONS
      YP(4)=0.0
      IF(CES(19,PLATE).GT.0.0) YP(4)=-CES(19,PLATE)*DST*(FSM -
     1 CES(20,PLATE))*FSM*VETAU
C
C     PLASTIC DEFORMATION RATE
      YP(5)=0.5*CES(8,PLATE)*DST*FSM*VETAU*P33
C
C     ENERGY EQUATION - (TEMPERATURE)
C     CONSISTENT UNITS USED IN ENERGY EQUATION
C     SPECIFIC HEAT MUST BE IN UNITS OF  DYNE-CM/GM/DEG C
      YP(6)=0.0
      DIVQ=0.
      RADIATE=0.
      IF(CES(30,PLATE).LT. 1.0)GO TO 30
      AKAPRM=-CES(5,PLATE)*CES(7,PLATE)
      IF(AKAP.LE.0.0)AKAPRM=0.0
      DENOM=(1.-DMG)*(CES(32,PLATE)*CES(1,PLATE)-CES(31,PLATE)*
     1 CES(31,PLATE)*AKAP*CES(30,PLATE))
```

```
      TEM0=CES(1,PLATE)*(1.-DMG)*(1.+2.*EPS11+EPS33)*RADIATE
      TEM1=0.9*(T33-QT-T11)*YP(5)/P33
      TEM2=3.*CES(31,PLATE)*AKAP*CES(30,PLATE)*(2.*E11*(YP(5)/2./P33 -
     1 YP(2)/3./(1.-DMG)) - E33*((RN-R)/DELTIM/DENS+YP(5)/P33+YP(2)/3./
     2 (1.-DMG)))
      TEM3=3.*CES(31,PLATE)*CES(30,PLATE)*(AKAPRM+AKAP/(1.-DMG))*(
     1 2.*EPS11+EPS33) -CES(31,PLATE)*CES(31,PLATE)*AKAPRM*
     2 (1.-DMG)*CES(30,PLATE)*(THETA -CES(30,PLATE))-(SIG-QT)/(1.-DMG)
      YP(6)=(DIVQ+TEM0+TEM1-TEM2-TEM3*YP(2))/DENOM
30    CONTINUE
      YP(7)=RADIATE-DIVQ/DENS-(T33-QT)*(RN-R)/DELTIM/DENS/DENS
      RETURN
      END
```

APPENDIX C

ADDITIONAL UPDATES FOR WONDY IV

```
*D WON.277,282
      JVN=J+12
      JDMG=J+13
      JDST=J+14
      JP33=J+16
      JTEMPR=J+17
      WRITE (21,1089) L,STORE(JX),STORE(JU),STORE(JR),STORE(JS),
     1 STORE(JDST),STORE(JVN),STORE(JDMG),STORE(JP33),STORE(JTEMPR)


*I WON.303
      WRITE (21,2001) CES(42,20)
 2001 FORMAT(/,10X,*CUMULATIVE DERIVATIVE CALLS FROM STEP1 =*,F18.1)


*D WON.447,449
     1/,*   L       POSITION      VELOCITY        DENSITY         STRESS
     2 DISLOC DENS VOID NO DENS       DAMAGE    LNG DEF GRAD  TEMPERATURE*
     3 ,/)
 1089 FORMAT(I6,6E14.5,3F12.6)


*D ONEDY.1907,1909
C     STRESS
      PLTS(L)=STORE(J+7)
C     VOID NUMBER DENSITY
      PLTR(L)=STORE(J+12)
C     DAMAGE  VOID VOLUME FRACTION
      PLTE(L)=STORE(J+13)
```

Appendix D

Table 1 - Data for fused quartz:

$\rho_o = 2.2$ gm/cm^3 $\quad C_o = 5.9391\ (10^5)$ cm/s $\quad \Gamma_o = 0.035$

Hugoniot - $P_H = \kappa_o \epsilon (1 + k_1 \epsilon + k_2 \epsilon^2 + k_3 \epsilon^3)$

$\kappa_o = \rho_o C_o^2 \quad k_2 = 39.098$

$k_1 = -5.3595 \quad k_3 = -89.252$

ϵ is the strain

Table 2 - Initial data for 1100 aluminum:

$\rho_R = 2.71$ gm/cm^3

$C_d = 6.365\ (10^5)$ cm/s

$\mu_o = 2.77\ (10^{11})$ dynes/cm^2

$\nu_o = 0.3313$

$B = 2.86\ (10^{-8})$ cm

$m = 2$

$\tau^* = 2.0\ (10^9)$ dynes/cm^2

$\tau(A_o) = 3.0\ (10^8)$ dynes/cm^2

$\gamma_o = 1.0\ (10^5)$

$1/n = 1$

DSTZ = $6.0\ (10^8)$

$A^* = 1.0\ (10^{-4})$

$C_h = 6\ (10^9)$/s/cm^3

$\sigma_1 = 4\ (10^8)$ dynes/cm^2

$\sigma_h = 3\ (10^9)$ dynes/cm^2

$\upsilon_o = 2.32\ (10^{-11})$ cm^3

$C_G = 0.00225$ cm^2/dyne/s

$\sigma_G = 3\ (10^9)$ dynes/cm^2

EPS = $1.0\ (10^{-4})$

$\theta_R = 300°K$

$\alpha = 2.3\ (10^{-5})$/°C

$C_t = 9.17\ (10^6)$ dyne cm/gm°C

Table 2 (Continued)

$D^*_{(T)} = 1.0\ (10^{10})$

FSMZ = 1.0

$B^* = -1.0$

$f^*_{(m)} = 1.0$

Table 3 - Second damage parameter set:

$C_h = 3\ (10^9)/s/cm^3$	$\upsilon_o = 2.32\ (10^{-11})\ cm^3$
$\sigma_l = 1\ (10^7)$ dynes/cm^2	$C_G = 4\ (10^{-4})\ cm^2/dyne/s$
$\sigma_h = 8\ (10^9)$ dynes/cm^2	$\sigma_G = 1\ (10^9)$ dynes/cm^2

UNLIMITED RELEASE

DISTRIBUTION:

Lynn Seaman
Stanford Research Institute
Menlo Park, CA 94025

D. R. Curran
Stanford Research Institute
Menlo Park, CA 94025

D. A. Shockey
Stanford Research Institute
Menlo Park, CA 94025

Tony E. P. Chen
Dept. of Mech. Eng. & Mech.
Lehigh University
Bethlehem, PA 18015

R. M. Schmidt
M. S. 4237
Boeing Aerospace
P. O. Box 3999
Seattle, WA 98124

J. Bridwell
Los Alamos Scientific Laboratory
P. O. Box 1663
Los Alamos, NM 87545

William J. Carter, M-6
Los Alamos Scientific Laboratory
P. O. Box 1663
Los Alamos, NM 87545

Charles L. Mader, T-4
Los Alamos Scientific Laboratory
P. O. Box 1663
Los Alamos, NM 87545

5000 A. Narath
Attn: 5200 E. H. Beckner
5400 A. W. Snyder
5700 J. H. Scott
5800 R. S. Claassen
5100 J. K. Galt
Attn: 5110 F. L. Vook
5120 G. J. Simmons
5130 G. A. Samara
5150 J. E. Schirber
5122 L. F. Shampine
5122 M. K. Gordon
5131 L. W. Davison
5131 J. W. Nunziato
5160 W. Herrmann
5162 L. D. Bertholf
5162 M. E. Kipp (15)
5162 R. J. Lawrence
5163 D. E. Munson
5163 K. W. Schuler
5166 A. J. Chabai
5166 P. Yarrington
5167 B. M. Butcher
5734 A. L. Stevens (8)
8266 Tech. Library (2)
3141 Tech. Library (5)
3151 Tech. Writing (3)
For ERDA/TIC (Unlimited Release)
ERDA/TIC (25)
(R. P. Campbell 3171-1)